PREDICTION OF FLOW RESISTANCE USING ARTIFICIAL NEURAL NETWORK (ANN) IN NATURAL VEGETATED CHANNEL

NUR ZAHIDAH BINTI KAMARUDZAMAN

CIVIL ENGINEERING
UNIVERSITI TEKNOLOGI PETRONAS

SEPTEMBER 2016

Prediction of Flow Resistance using Artificial Neural Network (ANN) in Natural Vegetated Channel

by

Nur Zahidah Binti Kamarudzaman
17417

Dissertation submitted in partial fulfillment of

the requirements for the
Bachelor of Engineering (Hons)
(Civil Engineering)

SEPTEMBER 2016

Universiti Teknologi PETRONAS,
32610, Bandar Seri Iskandar,
Perak Darul Ridzuan

CERTIFICATION OF APPROVAL

Prediction of Flow Resistance using Artificial Neural Network (ANN) in Natural Vegetated Channel
by

Nur Zahidah Binti Kamarudzaman

17417

A project dissertation submitted to the

Civil Engineering Programme

Universiti Teknologi PETRONAS

in partial fulfillment of the requirement for the

BACHELOR OF ENGINEERING (Hons)

(CIVIL ENGINEERING)

Approved by,

_____

(Associate Professor Dr. Khamaruzaman Wan Yusof)

UNIVERSITI TEKNOLOGI PETRONAS

BANDAR SERI ISKANDAR, PERAK

September 2016

CERTIFICATION OF ORIGINALITY

This is to certify that I am responsible for the work submitted in this project, that the original work is my own except as specified in the references and acknowledgments, and that the original work contained herein have not been undertaken or done by unspecified sources or persons.

_____

NUR ZAHIDAH BINTI KAMARUDZAMAN

Abstract

Naturally, vegetated channel has been developed for attenuating the flow in the drainage system. This is considered important as it will work as one of the effective ways to prevent high outflow velocity that could cause flooding and overtop of water at the outflow. The attenuated flow are as the result of the flow-resistant that existed within the drainage system and is manually calculated using Manning's Roughness Equation, where $V = \frac{Q}{A} = \frac{1}{n} R^{\frac{2}{3}} S^{\frac{1}{2}}$. Therefore, experiment procedure is established to obtain the Manning Roughness's Coefficient and from that, the experiment is conducted. The reading were taken at three main points. The reading were upstream of the natural vegetated channel, at the center of the natural vegetated region, and at the downstream of the natural vegetated channel. The Manning's Roughness Coefficient is then evaluated using Manning's Roughness Equation. On the basis of the measured data, all the parameter are then inputting in the engineering tool, Artificial Neural Network (ANN) to predict the same flow resistant that calculated earlier. Even though the predicted Manning's Roughness Coefficient may show good agreement to the experimental data; however, sensible engineering judgement must be taken into consideration as the experimental works were done in a controlled parameter, a small-scale laboratory test. Nonetheless, the natural vegetated channel is good medium to attenuate flow giving greater Roughness Manning's Coefficient than the existing precast concrete channel.

Acknowledgement

This project is based on the group research of both Muhamad Mujahid Muhamad and myself under the supervision of Associate Profesor Dr. Khamaruzaman Wan Yusof. I am grateful to both of my research partner and supervisor for all their countless effort being poured into this project. They have encouraged me to keep on going with the project even some unfortunate circumstances took place during the period of Final Year Project II semester.

I also thank Amanina Amir, my Civil Engineering colleague for corporation and effort in studying and exchanges of information in regards to this project. Due to that, I managed to understand the application of Artificial Neural Network using Matlab within time. Hence, able to present the needed and expected result during the UTP SEDEX Engineering Competition. With her help, I also able to perform the needed experiment at Universiti Sains Malaysia REDAC center, Nibong Tebal.

Moreover, I have to thank my family and friends for their countless support and effort in order to make me understand the application of Matlab in this project. Special thanks to my mother, Faridah Aini, for her support. Shee had supplied enough fund for me to operate this project and keep it going until the end of this project. Without her, I will never be able to complete the Final Report of this project within time.

TABLE OF CONTENTS

LIST OF FIGURES

LIST OF TABLES

1.0 Introduction

1.1 Background

Major cities and town with the high populated area have many drainage systems that act as a channel to discharge any water during a downpour. However, the drainage system will lose it main purpose if the water volume increases way more than the channel volume capacity and subsequently the area will be flooded.

In more technical terms, Ching et al (2013) stated that flood is a phenomenon of high water flow that dominates the natural or artificial channel banks and extended over the flood plain and will become a hazard to the society. Therefore, the hazard could be reduced by having alternative mitigation measure that could create a flow resistance to the high velocity of water going towards the high populated area. Hence, a natural vegetation was proposed as a means to create the necessary flow attenuation to the outflow discharge of water.

Vegetation, as mentioned above, plays an essential role in a river bioengineering system. In this project, the vegetation is applied onto the naturally vegetated channel with the certain specification of bioengineering. Hence, it influences the flow structure and the discharge of the river system caused by the flow resistant created by the vegetation. This paper will show the application of vegetation in a river and apply it to a channel for flood protection in the high populated area. This research should be able to reduce flood or become a standard means for flood protection during the two Monsoons seasons in Malaysia which are Southwest Monsoon and Northeast Monsoon.

Large data observation shows that most serious flooding cases happened due to high rainfall as a result of Monsoons and storms. Flooding that caused by this type of weather is seasonal. Nonetheless, due to high flood victims, seasonal flooding will also be taken into account. According to Thorndhal et.al (2008), the most problematic elements that increase the chances of flooding is the available drainage system in Malaysia. The six causes of the flood as mentioned by Thorndhal et. Al (2008) can be referred in Table 1.1 below:
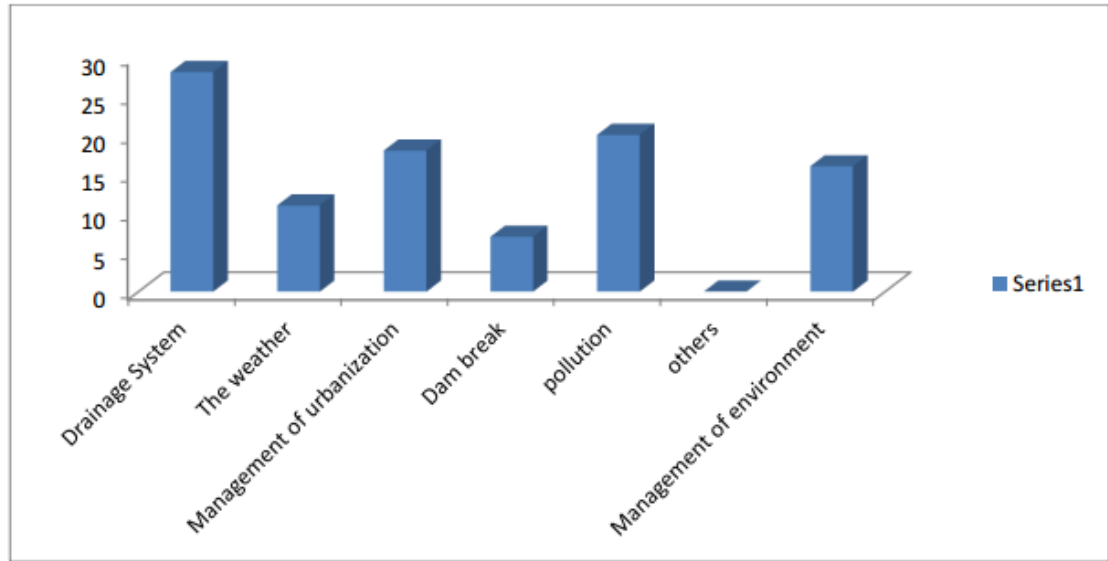
Figure 1.1.1: Causes of Flood

It is clear from Figure 1.1.1 above provided by Thorndhal et. Al (2008) that there is a serious need for improving our country's drainage system. From the chart, failure in the state's drainage system had cause to almost 30% flood cases. Therefore any improvement, however, is seen essential and can be made to the existing drainage characteristic such as improvement to the existing manning roughness coefficient, slope of the channel bed or improvement to the dimension of the open channel drainage system and this total improvement to the existing drainage system will reduce flood cases in Malaysia up to 30%.

To understand how serious is the problem during the flood, we will then observe the West Coast Flood Hydrograph below that is created using a set of data that were collected and analyzed by the Malaysia's Department of Irrigation and Drainage and were recorded in its Hydrological Procedure No. 27. The graph shows that the highest water discharged during a storm is 231.3 m^3/s. Which is considered high discharged value and may cause a flood and creates a hazard to the surrounding area. Therefore a medium, as proposed in the project, should be installed in a channel and should be able to create flow attenuation in order to reduce the flood.
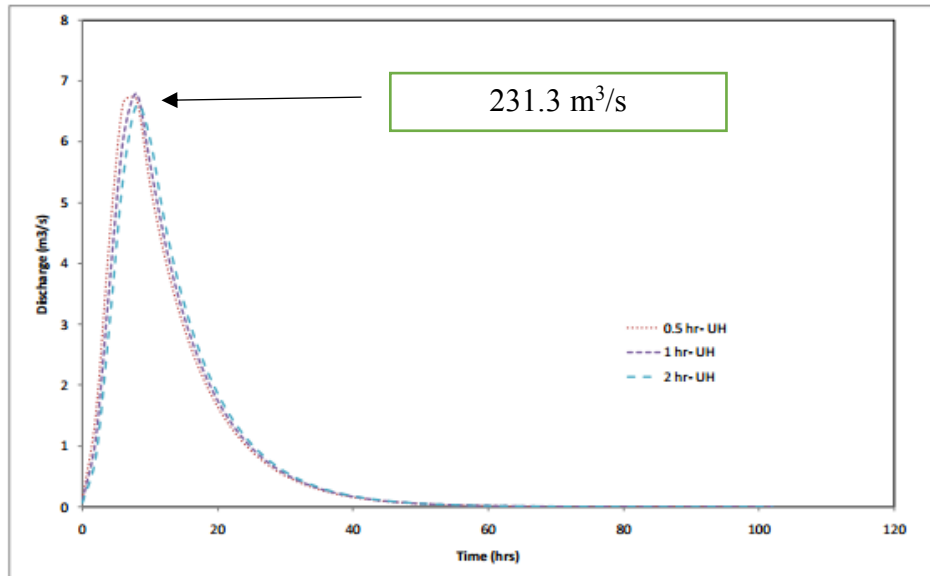
Figure 1.1.2: 0.5 Hour, 1 hour and 2-hour unit Hydrograph

Above tables resulted in the application of conventional concrete channel by the government agencies to overcome high runoff and flow. This is due to high degree of precision and confidence in precast concrete channel resulted in the usage of such concrete channel in the average drainage system. In engineering perspective, however, such application may result in sufficient protection to the related surrounding and no improvement have been made since the development of conventional concrete channel. Nonetheless, the conventional concrete channel resulted in 30% higher chances of flood causing an immediate assessment of the said conventional concrete channel. Therefore, a certain degree of questions should be answered whether or not the conventional concrete channel is still valid to be used in the increasing and rapid urbanization in the urban area.

Hence, improvement of the channel can be done using the bioengineering construction technique. In this project, the flow-resistant will be created by sets of vegetation that is installed in the channel. The proposed vegetation should be able to improve the existing drainage system characteristic by increasing the manning roughness coefficient subsequently reduce the velocity of the flow in a channel, creating flow attenuation and therefore be another form of flood protection to control the flooding in the affected area and will also be able to reduce flood cases in Malaysia up to 30%.

Bioengineering specification that is mentioned in the latter is the suitable construction method of the natural vegetated channel. In a more controlled surrounding, the bioengineering method should be seen as a viable method to counter flooding as well as reduces the pollution through soil infiltration and sedimentation. Therefore, not only reduces the chance of flooding but as well as increases the aesthetic value of a site and reduces the amount of pollution in our river system.

In this research, the bioengineering technique has been adopted using trial and error method. It is due to biotechnical engineering, that the trial and error method can be performed and the most suitable layout is able to produce the best result for Malaysia weather condition. Trial and error method can only be determined after a long through experiment and observation. Hence, therefore the adaptation of suitable bioengineering technique depended on the previous research papers and journals. Nonetheless, the experiment done in this project shows that the natural vegetated channel is able to become the alternative replacement for the existing conventional concrete channel.

1.2 Problem Statement

Flooding is considered to be the worst and most expensive natural disaster in Malaysia after landslides. The worst state affected by flooding in 2014 are Kelantan and Terengganu with 31 441 and 32 736 flood victims respectively and every year flooding cost the country about RM 1.50 billion (Jee Yee, T. 2015). The central government had to inject fund to the state affected by flood each year and the author saw this could be reduced by installing a naturally vegetated channel to reduce and create a flow attenuation to the discharge of the water flow by installing a velocity reduction medium. The reduced velocity of water flow will reduce the amount of water accumulate at the outlet and will significantly reduce flood at the affected area. Therefore enlighten the flooding situation. Currently, the reason of 30% flood probability is caused by the existing conventional concrete channel. From observation, it is seen that the improvement of channel needed an immediate attention due to the excessive urbanization that is currently ongoing and whether or not the existing conventional concrete channel is still viable to be applied in the current rapid urbanize area.

1.3 Objectives

The main objectives of this study are as follows:

1. To create a standard experimental procedure in determining the flow resistance of the naturally vegetated channel.
2. To predict the flow resistance using the artificial neural network (ANN).

1.4 Scope of Study

Vegetation in a channel creates a certain amount of flow-resistant in the channel that is able to be applied in Malaysia. If applied well, the vegetation in the channel could act as a flood control in the two states that are most affected by the flood which is Kelantan and Terengganu, especially during the Northeast Monsoon. Thus becoming one of the viable and alternative media in replacing the existing conventional concrete channel.

The vegetated channel is predicted to be able to reduce the flow attenuation and subsequently reduce the velocity of the water flow of the flood discharge and this is seen crucial when the flood discharge shows a high risk of flood hazard. Therefore the scope of this study is to be able to reduce flood by determining the flow resistance of the channel in order to create flow attenuation and once the flow resistance is sufficient, it should be able to control the flood situation when applied.

The scope of the study is to prove that the naturally vegetated channel is able to denote as the most viable and suitable alternative media in replacing the existing conventional concrete channel. Therefore the objectives of this paper should be met in order to be able to reduce the flooding situation in Malaysia when the experiment is applied to the potential high flooding area.

In this project, Adaptation of Manning Roughness Equation is being used to determine the Manning Roughness Coefficient of the naturally vegetated channel. The comparison will then be made to the existing conventional concrete channel and determine whether there is an improvement characteristic to the naturally vegetated channel. Further research is made by determining the suitable script from Matlab for determining the prediction of the Manning Roughness Coefficient.
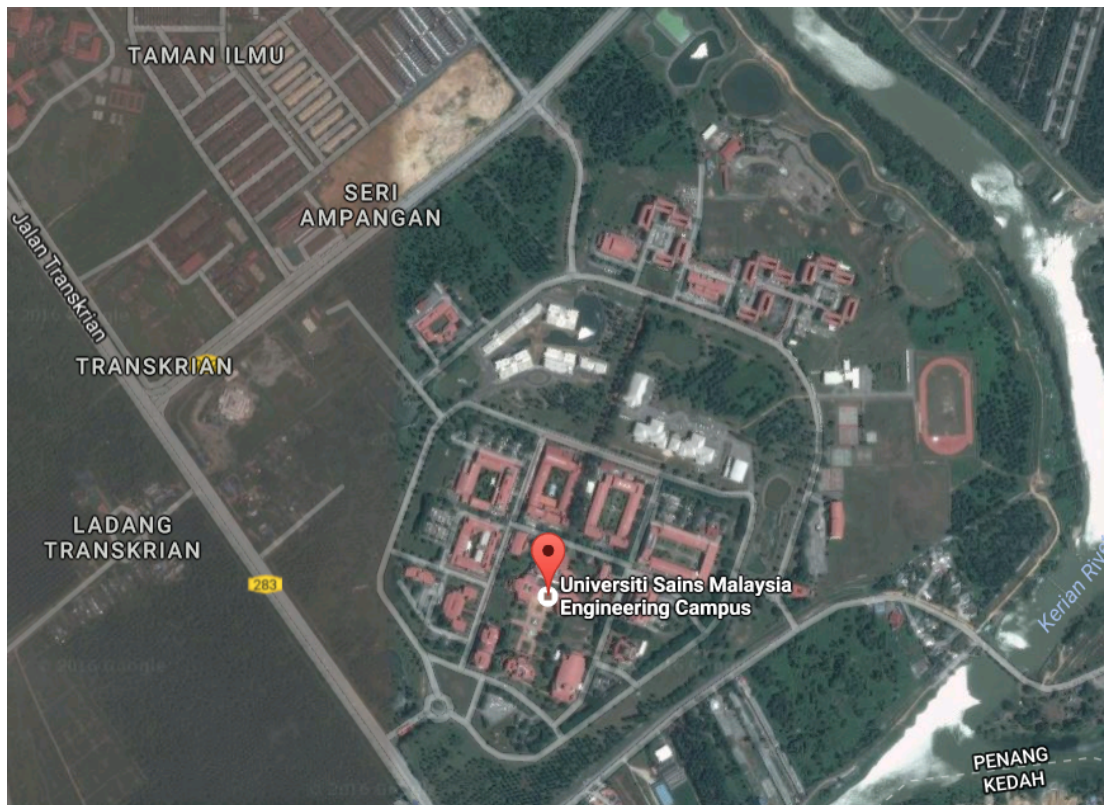
Figure 1.4.1: Maps of Universiti Sains Malaysia Engineering Campus

The experiment of this project will be done in Universiti Sains Malaysia REDAC center. The experiment will be done at the actual natural vegetated swale-type B and type C that is available at the surrounding site of the campus. The data collected is than analyze using Matlab. The study is considered as complete when the standard experimental procedure is established and the prediction is made with small amount of error.

2.0 Literature Review or Theory

Vegetated foreshores have been studied by Vulk, V et al (2016) and is seen effective to create wave attenuation. He studied that the naturally vegetated foreshores are able to create wave damping to the wave action of the coastal area during severe storm condition and from his studies, the author adapted that the same vegetation installation process could be applied to an open channel flow as shown in the image below. The vegetated channel should be able to create flow attenuation during severe Monsoons condition whereas mentioned before that severe flood discharge is 231.3 m^3/s as stated by the Department of Irrigation and Drainage Malaysia.

Figure 2.0: Natural Vegetated Channel in Universiti Sains Malaysia

2.1 Existing Drainage System

From Table 1.1 as mentioned before, the highest causes of the flood in Malaysia is due to the state's existing drainage system that fail to cater the high inflow velocity discharge during storm conditions. Thus, causing high-velocity outflow that may potentially result in flooding. Currently, the drainage system in Malaysia adapt an open channel system where every channel are precast with concrete Figure 2.1.1 below:

Figure 2.1.1: Precast open channel concrete drainage system

From observation, precast concrete for open channel drainage system does not provide the sufficient manning's roughness coefficient that could reduce the flow velocity. Hence create a high accumulation at the outflow of the channel at a short period of time, causing a sudden flood. Generally, manning's roughness coefficient for concrete provided by Universiti Sains Malaysia Urban Drainage Centre (Redac) is as Table 2.1.2 below:

Surface Cover or Finish	Suggested n values	
	Minimum	Maximum
Concrete		
Trowelled finish	0.011	0.015
Off form finish	0.013	0.018
Stone Pitching		
Dressed stone in mortar	0.015	0.017
Random stones in mortar or rubble masonry	0.020	0.035
Rock Riprap	0.025	0.030
Brickwork	0.012	0.018
Precast Masonry Blockwork	0.012	0.015

Table 2.1.2: Manning's Roughness Coefficient for precast concrete

From Table 2.1.2 above we conclude that the Manning Roughness Coefficient is not sufficient to create the necessary flow attenuation. Therefore, from the table, above we could improve the existing drainage system by increases the manning's roughness coefficient in order to achieve the sufficient flow velocity subsequently reduces the accumulation of outflow in a short period of time. For comparison purposes, Universiti Sains Malaysia also provides another Manning's Roughness Coefficient for grassed floodways as shown in Table 2.1.3 below:

Surface Cover	Suggested *n* values	
	Minimum	Maximum
Grassed Floodways		
Grass cover only		
Short grass	0.030	0.035
Tall grass	0.035	0.050
Shrub cover		
Scattered	0.050	0.070
Medium to dense	0.100	0.160
Tree cover		
Scattered	0.040	0.050
Medium to dense	0.100	0.120

Table 2.1.3: Manning's Roughness Coefficient for grassed floodways.

It is clear from Table 2.1.2 and Table 2.1.3 that there is an increment of Manning's Roughness Coefficient after the installation of vegetation in the open channel drainage system. This is essential and very much needed as the flood control measurement because sufficient Manning's Roughness Coefficient could decrease the flow velocity subsequently decreases the outflow discharge at the outflow of the open channel drainage system. Hence, the next step is to model the hydrology condition in ANN and obtain the predicted flow resistant of the naturally vegetated channel.

Even though by surface properties precast concrete channel has disadvantages due to its low Manning's Roughness Coefficient, however, it does have a longer lifespan and does not face channel erosion in short period of time as compared to a naturally vegetated channel. Therefore, the layout of the naturally vegetated channel has to be considered and analyzed as well so that optimum layout could be achieved in order for

it to work properly even in the experimental phase. Hence, the best layout would be to spread out some cobbles and stones at Q_1 as image 2 below:
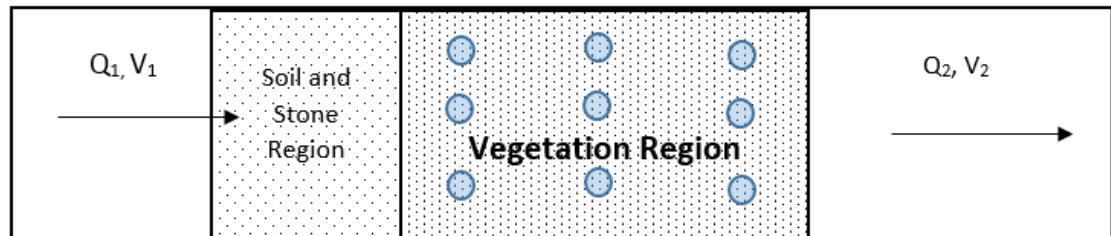
Figure 2.1.4: Plan View Arrangement Layout in a Flume

The purpose of the soil and stones region is to create a damping effect to the high inflow discharge and to avoid critical flow velocity so that the vegetation region will not be swept away by the flow of the water as well provide a good stable condition for the vegetation to grow within a period of time.

2.2 Manning's Equation

Manning's Equation is seen as viable to access the reliability of this experiment due to the type of parameters involved. The parameter that is linked closely to the experiment is the Manning's Roughness Coefficient. Manning's Roughness Coefficient took the roughness of the channel into accountability hence differentiate the roughness of the channel and the flow resistant created by the vegetation in the channel. Hence, giving a higher understanding towards the subject and yield a more accurate result.

Manning Equation were first derived from Chezy Equation where parameters involved are Chezy coefficient, C, Hydraulic Radius, R, and Slope of the channel, S. Chezy Equation mentioned above is as follows:

$$V = C\sqrt{R.S}$$

Manning, however, derived it further from including the roughness coefficient of the channel, n. Given that the empirical relation between Chezy equation and Manning Equation is as below:

$$C = \frac{1}{n} R^{1/6}$$

Therefore for better understanding the derivative of Manning's Equation from Chezy Equation would be:

$$V = (\frac{1}{n} R^{1/6}) R^{1/2} S^{1/2}$$

Subsequently, the equation is mathematically converted as below:

$$V = \frac{Q}{A} = \frac{1}{n} R^{\frac{2}{3}} S^{\frac{1}{2}}$$

Where
$V = Mean\ Velocity\ of\ Flow, {}^{m}/_{S}$
$n = Manning\ Roughness\ Coefficient$
$R = Hydraulic\ Radius, m$
$S = Slope\ of\ energy\ grade\ line, {}^{m}/_{m}$
$Q = Flow\ Rate\ Discharge, {}^{m^3}/_{S}$
$A = Flow\ Area\ of\ Channel, m^2$
$C = Chezy\ Coefficient$

The area, A and the Hydraulic Radius, R in Manning's Equation varies depended on the physical properties of the channel. The area, A and the Hydraulic Radius, R of the channel can be easily determined by the sets of formulae in the Table 2.2.1 below. However, in this research, we will use the rectangle channel physical properties as parameters.
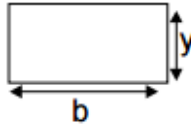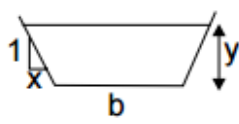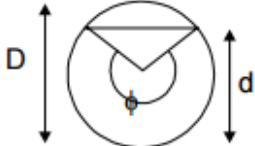
	Rectangle	Trapezoid	Circle
Area, A	by	$(b+xy)y$	$\frac{1}{8}(\phi - \sin\phi)D^2$
Wetted perimeter P	$b+2y$	$b+2y\sqrt{1+x^2}$	$\frac{1}{2}\phi D$
Top width B	b	$b+2xy$	$(\sin\phi/2)D$
Hydraulic radius R	$by/(b+2y)$	$\dfrac{(b+xy)y}{b+2y\sqrt{1+x^2}}$	$\dfrac{1}{4}\left(1-\dfrac{\sin\phi}{\phi}\right)D$
Hydraulic mean depth D_m	y	$\dfrac{(b+xy)y}{b+2xy}$	$\dfrac{1}{8}\left(\dfrac{\phi-\sin\phi}{\sin(1/2\phi)}\right)D$

Table 2.2.1: Different Type of Channel's Physical Properties

2.3 Artificial Neural Network (ANN)

Once all the experimental data are obtained through experimental works, the same experimental data and hydrology condition were then applied to Artificial Neural Network (ANN). A software or modeling that is designed to do some prediction in controlled parameters. By definition, Artificial Neural Network (ANN) is a computational model or a software that its product or output is dictated by structure and functions of biological neural networks, in this case, the parameters of the channel.

The Manning's Roughness Coefficient, *n* should match the experimental Manning's Roughness Coefficient obtained theoretically. Artificial Neural Network (ANN) is being chosen as the main software to model the condition of this experiment is because according to Muravyev et al (2016) an optimized Artificial Neural Network (ANN) should be able to approximate or predict any continuous non – linear function, being highly tolerant to any missing data or noises resulting to more trusted and accurate result. In general, the process of how Artificial Neural Network works is as progress flow below.
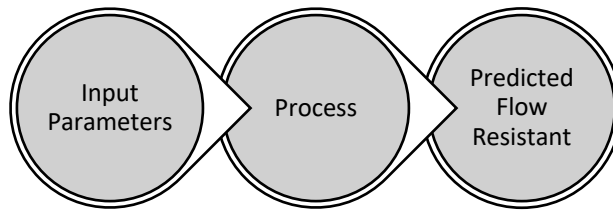
Figure 2.3.1: Progress Flow of Artificial Neural Network (ANN)

In this project, it is determined that the suitably hidden layer is the 10 whereas any hidden layer greater than 10 may result to overfitting of the results. The increment of hidden layer is by trial and error method whereby increment of hidden layer is depended on performance progress. Figure 2.3.2 below shows the Network Architecture of the Artificial Neural Network tool.
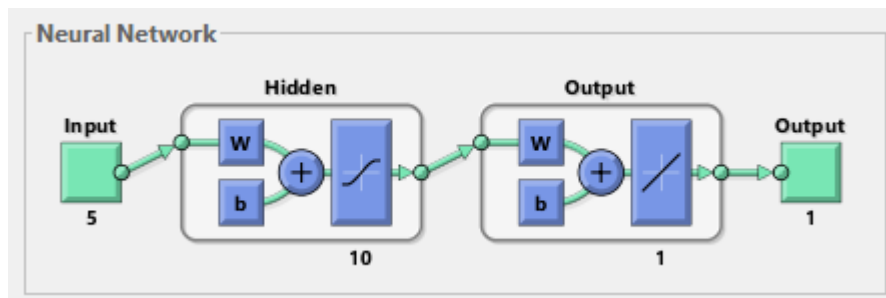
Figure 2.3.2: Network Architecture of the Artificial Neural Network

From the program being set by the Matlab, the training will be done using Lavenberg-Marquardt algorithm. The algorithm is also known as a damped least square method. The algorithm is seen suitable to be used in the Artificial Neural Network as it is able to analysis non-linear squares problem. The algorithms specifications used in Matlab is shown in Figure 2.3.3 below:
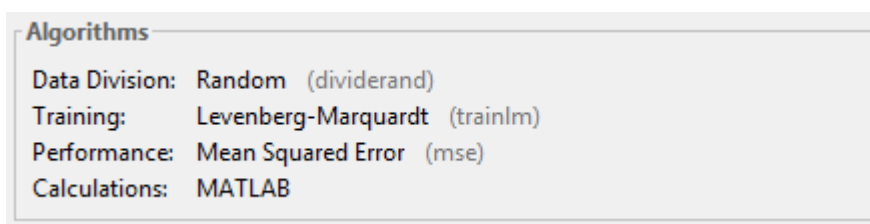
Figure 2.3.3: Algorithm Specifications used in Matlab

2.4 Reliability and accuracy of the experimental data

Reliability of the experimental data is very important and essential in this research as the data will going to be inputted into the Artificial Neural Network software. Any unreliable data will cause the software to produce unreliable result causing a misleading view and perception towards the experiment and the whole research. Therefore, according to Kee et al (n.d.) the reliability of the experiment and the prediction in the modeling, however, can be determined by the Root Mean Square Error, RMSE, and coefficient of determination, R^2. In general, Root Mean Square Error, RMSE is the variance, $\acute{O}$ of the whole experiment to determine the consistency and the accuracy of the obtained data. The equation that denotes the Root Mean Square Error and coefficient of determination of Manning's Equation are as follows:

$$Coefficient\ of\ Determination, R^2$$

$$= \left(\frac{\sum_{i=1}^{N}(O_i - O_{mean})(P_i - P_{mean})}{\sqrt{\sum_{i=1}^{N}(O_i - O_{mean})^2 \sum_{i=1}^{N}(P_i - P_{mean})^2}} \right)^2$$

$$Root\ Mean\ Square\ Error, RMSE = \sqrt{\frac{\sum_{i=1}^{N}(O_i - P_i)^2}{N}}$$

Where
$O_i = Observed\ Values$
$O_{mean} = mean\ of\ O_i$
$P_i = Predicted\ Values$
$P_{mean} = mean\ of\ P_i$
$N = number\ of\ samples$

Therefore from the said equation, the Artificial Neural Network (ANN) will predict the most accurate result when the calculated Root Mean Square Error, RMSE has the smallest value which denotes the smallest uncertainty. The prediction is also

considered correct when the coefficient of determination, R^2 is approaching to 1. The result is considered accurate enough when $R^2 \geq 0.7$.

2.5 Flow Attenuation

The inflow of water can be high at a time especially during stormy and rainy weather. The heaviest rainfall in Malaysia would be during the two Monsoons which are Southwest Monsoon and Northeast Monsoon. The high peak of inflow could result to high velocity in the drainage system and cause the risk of flood. Therefore the aim of this research is to create a flow attenuation which is defined as the reduction of hydrograph peak. Attenuation mentioned can be observed as the graph below.
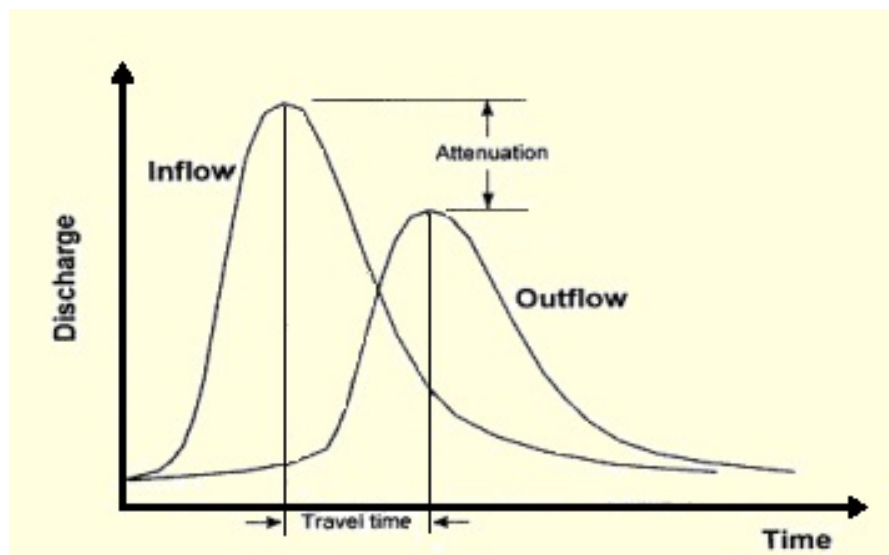
Figure 2.5.1: Flow Attenuation

To create flow attenuation, some flow resistant object has to be established to increase the roughness causing flow attenuation in the hydrograph. Therefore in this research, the subject that will be used to create flow resistant in the rectangle flume would be grass and this vegetation will be installed at the bottom of the channel. In this experiment, many types of grasses will be used to determine the different scales of flow-resistant in a certain hydrological condition (Sand-Jensen, 2003). The type of vegetation that will create optimum flow resistant should be able to be applied as a flood measurement control in Malaysia.

2.6 Advantage of bioengineering technique

The application of bioengineering techniques gives a lot of advantages in terms of biological, technical, aesthetic and economic. Their advantages make bioengineering technique as one of the techniques that are worth researching and expanding understanding of its characteristics. Not only it became the best tool for overcoming flood, but it also possesses the element of natural which is a great contribution to the aesthetic value. The natural cow grass that is being used not only inexpensive but can be obtained from anywhere within Malaysia. Not to mention it also considered being cheaper in production as compared to the existing conventional concrete channel. Table 2.6.1 below shows the advantages of the naturally vegetated channel in 4 aspects.

Aspects	Advantages
Technical	1. Become bank protection during flood 2. Become slope protection during heavy rainfall 3. Increase the stability of the channel by having soil-root bond of the vegetation
Ecological	1. Enhancing the habitat of the ecological system by reducing the amount of human-made structure 2. Improved the soil water condition by having infiltration, filtration and detention. 3. Soil enhancement by having humus formation 4. Creation of habitats other than the laid cow grass 5. Water purification
Aesthetical	1. Harmonize with the natural surrounding 2. Has the dimension of a river shape 3. Minimize the usage of human-made structure
Economical	1. Increases the amount of maintenance needed 2. Inexpensive material such as cow grass 3. Does not need excellent workmanship to create the design naturally vegetated channel

Table 2.6.1: Advantages of the Natural Vegetated Channel

2.7 Difference of Type B and Type C swale

In this project, the actual reading is being taken at the actual site of the grass swale that is situated in the surrounding of the Universiti Sains Malaysia Nibong Tebal campus. The reading is taken at two type of swale which is Type B and Type C grass swale. The swale is differentiated by the cross section of the swale and the bed slope of the grass swale as shown in Figure 2.7.1, Figure 2.7.2, Figure 2.7.3 and Figure 2.7.4 below.
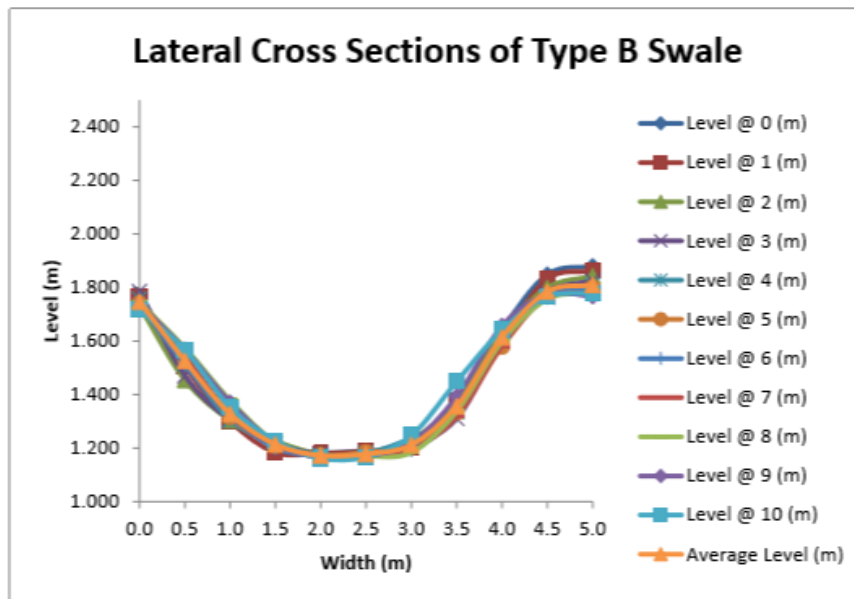
Figure 2.7.1 Cross Section of Type B Swale
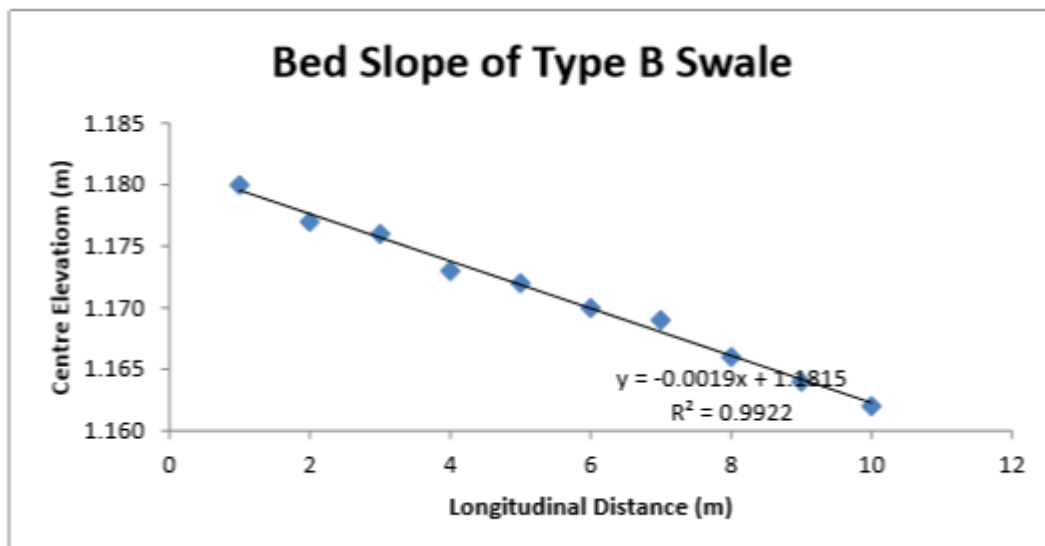
Figure 2.7.2: Bed Slope of Type B swale
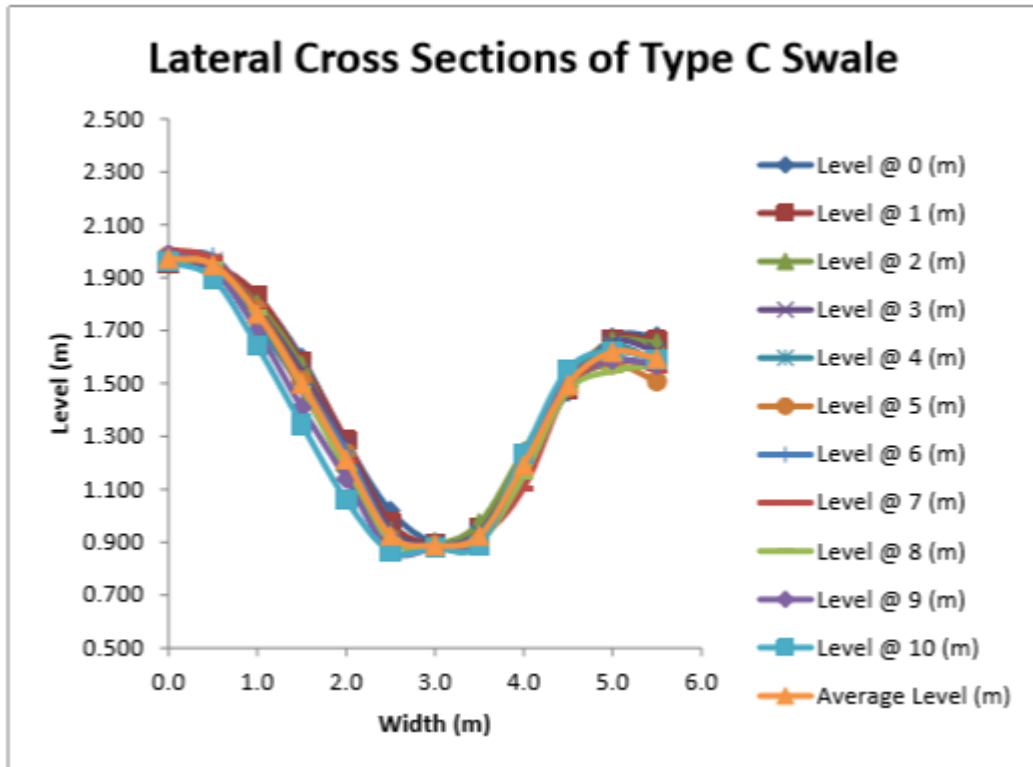
Figure 2.7.3: Cross Section of Type C Swale
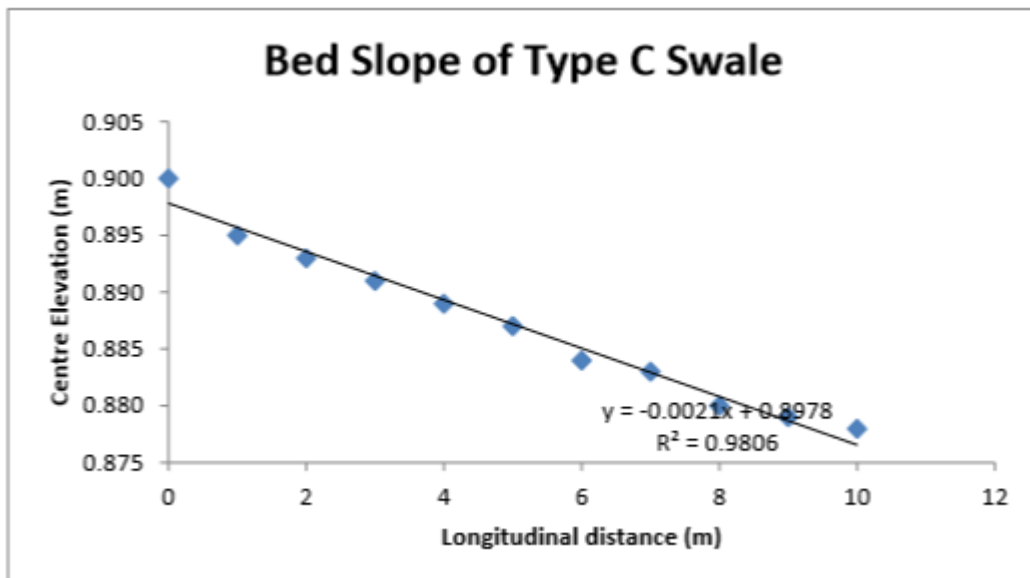
Figure 2.7.4: Bed Slope of Type C Swale

3.0 Methodology / Project Work

For project work, the experiment will be held at Physical Modelling Laboratory of River Engineering and Urban Drainage Research Centre (REDAC) at Universiti Sains Malaysia. One of the equipment that we will use at the research center is the flume that could control the parameters of desired hydrology condition. The diagram of the flume with the vegetation zone that we will establish in this research would be as follows:
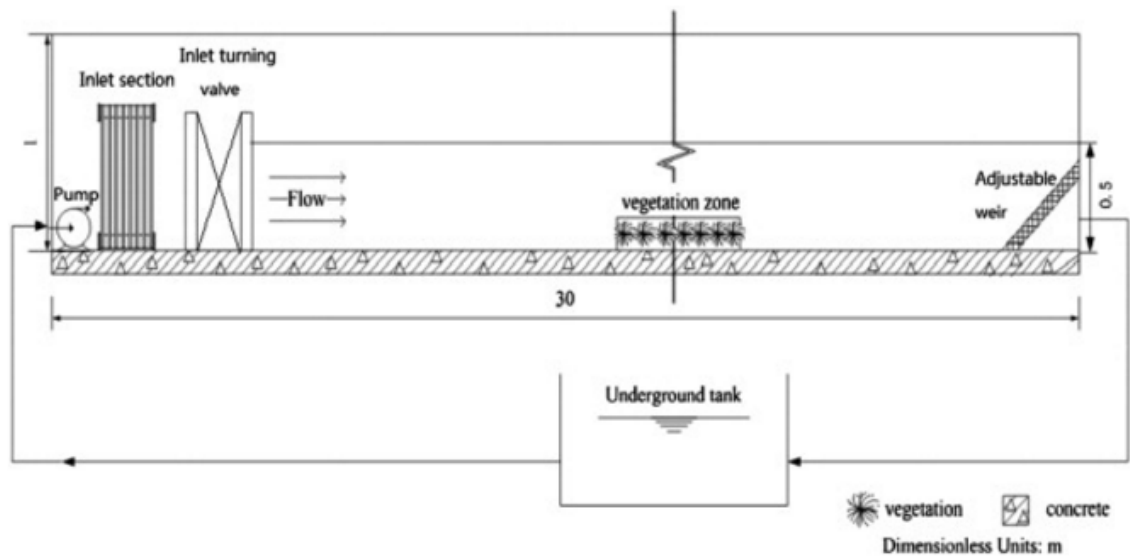
Figure 3.1 Side View Arrangement Layout in a Flume
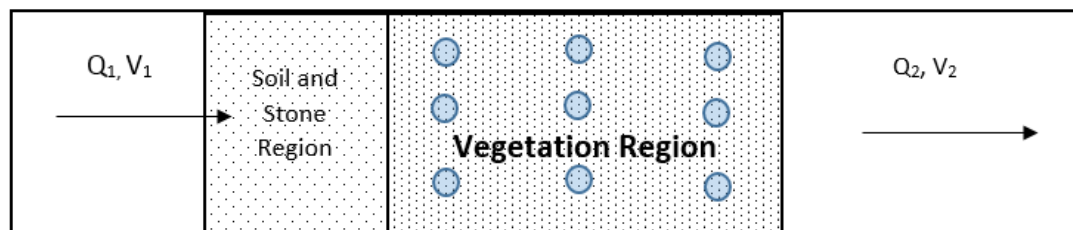
Figure 3.2 Plan View Arrangement Layout in a Flume

Where

→ = Water direction

Q_1 = Discharge of water into the Rectangular Channel
Q_2 = Discharge of water out from the Rectangular Channel
V_1 = Velocity of water flow into the Rectangular Channel
V_2 = Velocity of water flow out from the Rectangular Channel
○ = Potential reading point for Velocity reading
▢ = Soil and Stone Region act as stabilizer for the vegetation region
▢ = Vegetation Region that act as flow resistant

The first step in this experiment is to determine the Manning's Roughness Coefficient of the non-vegetation in the flume. The non-vegetation flume condition will act as the base and the control parameters of the hydrology condition. Later then, the vegetation region is then added into the flume to observe and record the increment of the Manning's Roughness Equation. Once recorded and new Manning's Roughness Coefficient is established, the modeling and the prediction of the flow-resistant in Artificial Neural Network (ANN) can be done. Generally, the flow of the experiment will be conducted using the Figure 3.3 below.
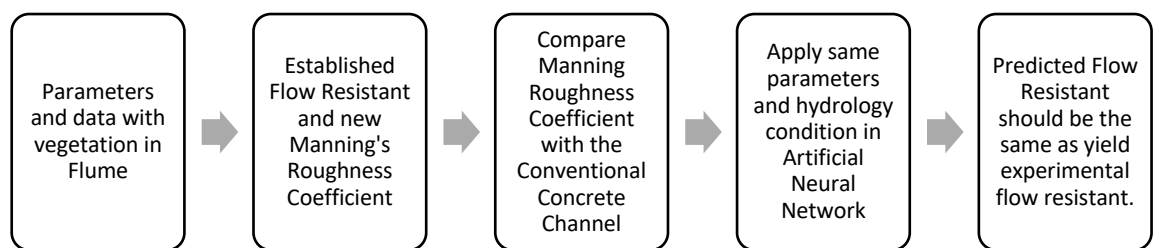
Figure 3.3: Flow of the Experiment

Therefore any increment of Manning's Roughness Equation will be safely deducted as flow resistant of the vegetation. The control base Manning's Roughness Equation can be calculated using the equation below:

$$n = \frac{1}{V} R^{2/3} S^{1/2}$$

In this experiment, the parameters that will be taken account is the slope of the flume, S, the velocity of the flow, V, and the hydraulic radius, R of the flume. The table below will be used in both non-vegetation and vegetation condition when doing the experimental works.

Flume Without Vegetation						
Width of Flume (mm)	Slope, S	Hydraulic Radius, R	Depth, d (m)	Velocity of the Water Flow, V	Average Velocity of Water Flow, V	Manning's Roughness Coefficient, n
	0.0010		0.2d			
			0.6d			
			0.8d			
	0.0015		0.2d			
			0.6d			
			0.8d			
	0.0020		0.2d			
			0.6d			
			0.8d			
Flume With Vegetation						
	0.0010		0.2d			
			0.6d			
			0.8d			
	0.0015		0.2d			
			0.6d			
			0.8d			
	0.0020		0.2d			
			0.6d			
			0.8d			

Table 3.4: Data Collection Sheet

Once the experiment data are all collected and calculated, the Root Mean Square Error, RMSE and the Coefficient of Determination, R^2 is then calculated as per equations below to determine the accuracy of the data before being inputted into the Artificial Neural Network (ANN) software.

$$Coefficient\ of\ Determination, R^2$$

$$= \left(\frac{\sum_{i=1}^{N}(O_i - O_{mean})(P_i - P_{mean})}{\sqrt{\sum_{i=1}^{N}(O_i - O_{mean})^2 \sum_{i=1}^{N}(P_i - P_{mean})^2}} \right)^2$$

$$Root\ Mean\ Square\ Error, RMSE = \sqrt{\frac{\sum_{i=1}^{N}(O_i - P_i)^2}{N}}$$

Once the reliability of the experimental data is confirmed yielding small value of Root Mean Square Error, RMSE, and Coefficient of Determination, $R^2 \geq 0.7$, then the same hydrology conditions will be applied to the Artificial Neural Network to predict the flow resistant at any slope and velocity of the water flow.

4.0 Results and Discussion

In this project, there will be two results to entertain both of the objectives of this study. The objectives are:

1. To create a standard experimental procedure in determining the flow resistance of the naturally vegetated channel.
2. To predict the flow resistance using the artificial neural network (ANN).

4.1 Standard Experimental Procedure
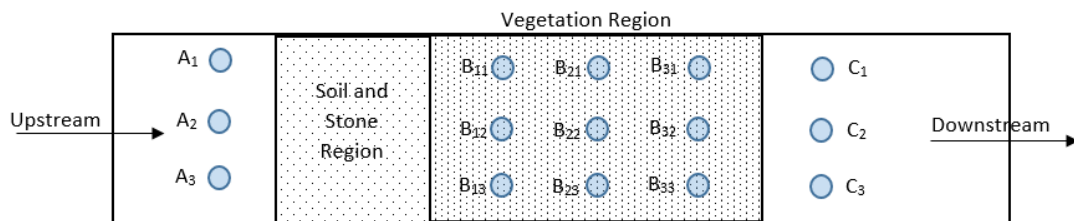
Figure 4.1.1: Plan View Arrangement Layout in a Flume

Where

$\rightarrow$ = Water direction

Q_1 = Discharge of water into the Rectangular Channel

Q_2 = Discharge of water out from the Rectangular Channel

V_1 = Velocity of water flow into the Rectangular Channel

V_2 = Velocity of water flow out from the Rectangular Channel

$\bigcirc$ = Potential reading point for Velocity reading

$\square$ = Soil and Stone Region act as stabilizer for the vegetation region

$\square$ = Vegetation Region that act as flow resistant

Therefore, from the layout given above, the standard experimental procedure that should be carefully considered in order to achieve the objective of this experiment are as follows:

1. Establish 5 m length of vegetation region with 1.5 m width.
2. The thickness of the vegetation region should approximately be up to 7.62 cm (3 inches) as shown in the image below. However, the thickness of the vegetation must be taken into consideration when the thickness of the vegetation is much smaller than the annual rainfall of the potential site.
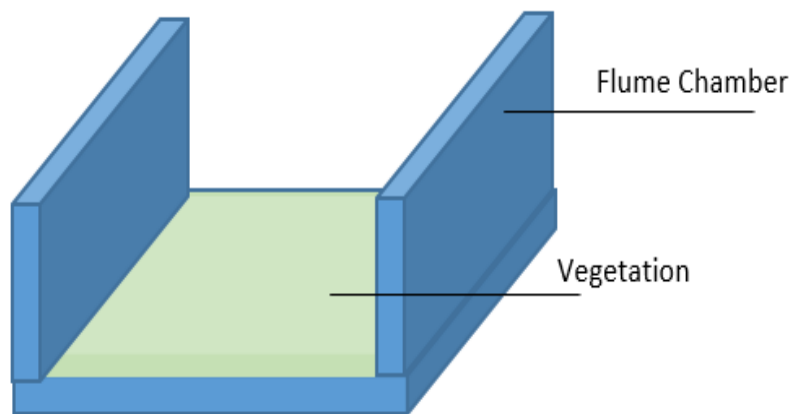
Figure 4.1.2: Cross section of naturally vegetated channel

3. Run the 20 m flume with three different water depth, 10 cm, 20 cm, and 30cm.
4. With each water depth, the reading will be taken at three different slopes. In other words, Slope of 1000, 750 and 500 will be tested at 10 cm, 20 cm, and 30 cm water depth.
5. Once the flume reaches the desired water depth, velocity reading will be taken at the upstream of the vegetated region, Point A. Velocity reading at Point A_1, A_2 and A_3 for all 0.2y, 0.4y, and 0.6y depth are taken and must consider the drag force effect of the flume to the water flow. It is expected that point A_2 should yield greater velocity than at point A_1 and point A_3. Image below shows the relationship of the surface to the water flow.

All surface with certain degree of roughness will result to lowering of velocity of the water flow

0.4 m/s

0.3 m/s

0.2 m/s

0.1 m/s

0.05 m/s
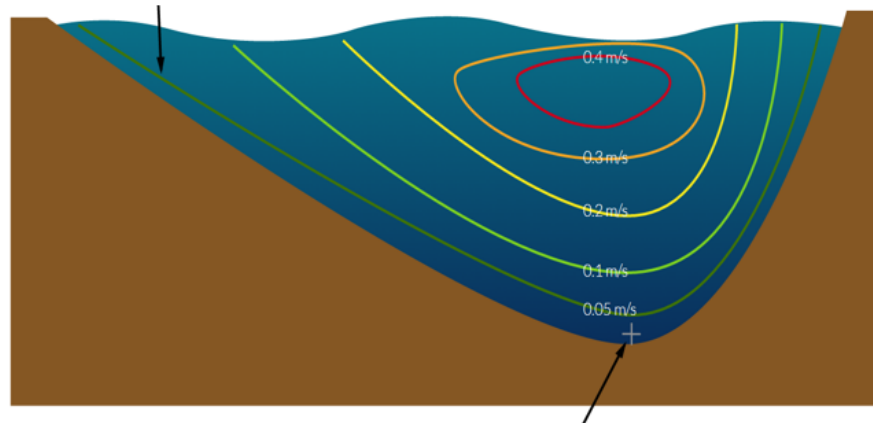
Figure 4.1.3: Effect of Manning Roughness Coefficient of the surface to the water flow velocity.

6. Next, velocity reading will be taken at the downstream of the vegetated region, Point C. Velocity reading at Point C_1, C_2 and C_3 for all 0.2y, 0.4y and 0.6y depth are taken and again must consider the drag force effect of the flume to the water flow. It is expected that point C_2 should yield greater velocity than at point C_1 and point C_3.

7. Velocity reading at $B_{11\text{-}13}$, $B_{21\text{-}23}$ and $C_{31\text{-}33}$ is then taken at the vegetation region. All velocity reading at point B is taken at 0.2y, 0.4y and 0.6y depth and again must consider the drag force effect of the flume to the water flow.

8. The drag effect of the flume to the water flow, also known as Manning's Roughness Coefficient, is then calculated using Manning's Roughness Equation.

9. The increment of Manning's Roughness Coefficient is then observed at all Point A, B and C. Provided that flume material does not change, Manning's Roughness Coefficient at Point A and C will remain constant and changes in velocity at Point C is as the result of Manning's Roughness Coefficient increment at Point B.

10. The Same procedure is then repeated through steps 1 till 9 in an empty flume and this will act a control parameter of the experiment.

11. The Same parameter is then inputted in Artificial Neural Network to obtain the desired flow resistant as done in the experiment laboratory test.

4.2 Data Collection and Calculation for Type B Swale

The result is taken at both of the upstream and the downstream part of the grass swale. The data collected at the upstream and downstream of the grass swale is as shown in Table 4.2.1 and Table 4.2.2 below. The Manning Roughness Coefficient is calculated using Roughness Manning Equation as shown in section 2.0.

			Upstream in Swale Type B			
Time	Average Velocity	Depth	Area	Wetted Perimeter	Hydraulic Radius	Manning Roughness, n
1000	0.364	0.430	0.850	3.136	0.271	0.051
1100	0.140	0.370	0.670	2.797	0.240	0.123
1200	0.087	0.340	0.665	3.063	0.217	0.186
1300	0.059	0.350	0.590	2.708	0.218	0.275
1400	0.065	0.300	0.550	2.606	0.211	0.244
1500	0.058	0.280	0.530	2.610	0.203	0.265
1000	0.160	0.360	0.802	2.967	0.270	0.117
1100	0.122	0.350	0.641	2.633	0.243	0.142
1200	0.119	0.330	0.651	2.798	0.233	0.142
1300	0.098	0.330	0.627	2.825	0.222	0.167
1400	0.054	0.280	0.540	2.671	0.202	0.284
1500	0.071	0.280	0.535	2.488	0.215	0.226
1800	0.194	0.320	0.695	2.557	0.272	0.097
1800	0.072	0.270	0.634	3.262	0.194	0.209

Table 4.2.1: Upstream data in Type B Swale

			Downstream in Swale Type B			
Time	Average Velocity	Depth	Area	Wetted Perimeter	Hydraulic Radius	Manning Roughness, n
1000	0.562	0.330	0.550	3.062	0.180	0.025
1100	0.194	0.230	0.404	2.471	0.164	0.069
1200	0.211	0.210	0.380	2.537	0.150	0.060
1300	0.148	0.220	0.340	2.531	0.134	0.079
1400	0.107	0.120	0.165	2.143	0.077	0.076
1500	0.102	0.180	0.255	2.522	0.101	0.095
1000	0.119	0.260	0.468	2.648	0.177	0.119
1100	0.146	0.200	0.402	2.450	0.164	0.092
1200	0.042	0.250	0.387	2.451	0.158	0.310
1300	0.041	0.220	0.402	2.457	0.163	0.323
1400	0.052	0.230	0.343	2.382	0.144	0.238
1500	0.061	0.230	0.325	2.521	0.129	0.187
1800	0.292	0.230	0.445	2.836	0.157	0.045
1800	0.096	0.220	0.445	2.838	0.157	0.136

Table 4.2.2: Downstream data in Type B Swale

From the table, it is shown that the upstream accommodate more flow area as compared to the downstream of the grass swale. From observation, the upstream has lower velocity reading as compared to the downstream data. This is as a result due to the increment of Roughness Manning Coefficient and blockade capacity of the naturally vegetated channel. In this regards, it is shown that in Table 4.2.3 below that the flow discharge decreases within time. Hence, it is known that the effect of an increment of Manning Roughness Coefficient took place.

Time	Upstream			Downstream		
	Average Velocity	Area	Discharge, Q	Average Velocity	Area	Discharge, Q
1000	0.364	0.850	0.309	0.562	0.550	0.309
1100	0.140	0.670	0.094	0.194	0.404	0.078
1200	0.087	0.665	0.058	0.211	0.380	0.080
1300	0.059	0.590	0.035	0.148	0.340	0.050
1400	0.065	0.550	0.036	0.107	0.165	0.018
1500	0.058	0.530	0.031	0.102	0.255	0.026
1000	0.160	0.802	0.128	0.119	0.468	0.056
1100	0.122	0.641	0.078	0.146	0.402	0.059
1200	0.119	0.651	0.077	0.042	0.387	0.016
1300	0.098	0.627	0.061	0.041	0.402	0.016
1400	0.054	0.540	0.029	0.052	0.343	0.018
1500	0.071	0.535	0.038	0.061	0.325	0.020
1800	0.194	0.695	0.135	0.292	0.445	0.130
1800	0.072	0.634	0.046	0.096	0.445	0.043

Table 4.2.3: Flow Discharge of the Upstream and the Downstream of Type B Swale

4.3 Data Collection and Calculation for Type C Swale

Similar to data collection procedure in Type B grass swale, the result is taken at both of the upstream and the downstream part of the grass swale. The data collected at the upstream and downstream of the grass swale is as shown in Table 4.3.1 and Table 4.3.2 below. The Manning Roughness Coefficient is calculated using Roughness Manning Equation as shown in section 2.0.

Upstream in Swale Type C						
Time	Average Velocity	Depth	Area	Wetted Perimeter	Hydraulic Radius	Manning Roughness, n
700	0.139	0.170	0.085	0.500	0.170	0.099
800	0.097	0.160	0.080	0.500	0.160	0.136
900	0.086	0.160	0.080	0.500	0.160	0.153
1000	0.083	0.160	0.080	0.500	0.160	0.158
1100	0.092	0.160	0.780	0.500	0.155	0.141
1200	0.100	0.190	0.093	0.500	0.185	0.145
1300	1.725	0.390	0.195	0.500	0.390	0.014

Table 4.3.1: Upstream Data in Type C Swale

Downstream in Swale Type C						
Time	Average Velocity	Depth	Area	Wetted Perimeter	Hydraulic Radius	Manning Roughness, n
700	0.178	0.150	0.075	0.500	0.150	0.071
800	0.111	0.130	0.065	0.500	0.130	0.103
900	0.103	0.140	0.070	0.500	0.140	0.117
1000	0.061	0.110	0.055	0.500	0.110	0.168
1100	0.044	0.120	0.058	0.500	0.115	0.238
1200	0.083	0.150	0.075	0.500	0.150	0.152
1300	1.675	0.350	0.175	0.500	0.350	0.013

Table 4.3.2: Downstream Data in Type C Swale

From the table, it is shown that the upstream accommodate more flow area as compared to the downstream of the grass swale. From observation, the upstream has lower velocity reading as compared to the downstream data. This is as a result due to the increment of Roughness Manning Coefficient and blockade capacity of the naturally vegetated channel. In this regards, it is shown that in Table 4.3.3 below that the flow discharge decreases within time. Hence, it is known that the effect of an increment of Manning Roughness Coefficient took place.

	Upstream			Downstream		
Time	Average Velocity	Area	Discharge, Q	Average Velocity	Area	Discharge, Q
700	0.139	0.085	0.012	0.178	0.075	0.013
800	0.097	0.080	0.008	0.111	0.065	0.007
900	0.086	0.080	0.007	0.103	0.070	0.007
1000	0.083	0.080	0.007	0.061	0.055	0.003
1100	0.092	0.780	0.072	0.044	0.058	0.003
1200	0.100	0.093	0.009	0.083	0.075	0.006
1300	1.725	0.195	0.336	1.675	0.175	0.293

4.4 Regression Analysis for Both Type-B Upstream and Downstream Data

Regression analysis is the statistical modeling of a range of data and to prove that the data is within the limit of Root Mean Square Error and Coefficient of Determination, R^2. It is known that a good data should have Coefficient of Determination, R^2 approaching to 1. From the Regression Analysis done by Matlab using Artificial Neural Network, the average Coefficient of Determination, R^2 for Upstream Data is $R^2 = 0.99546$
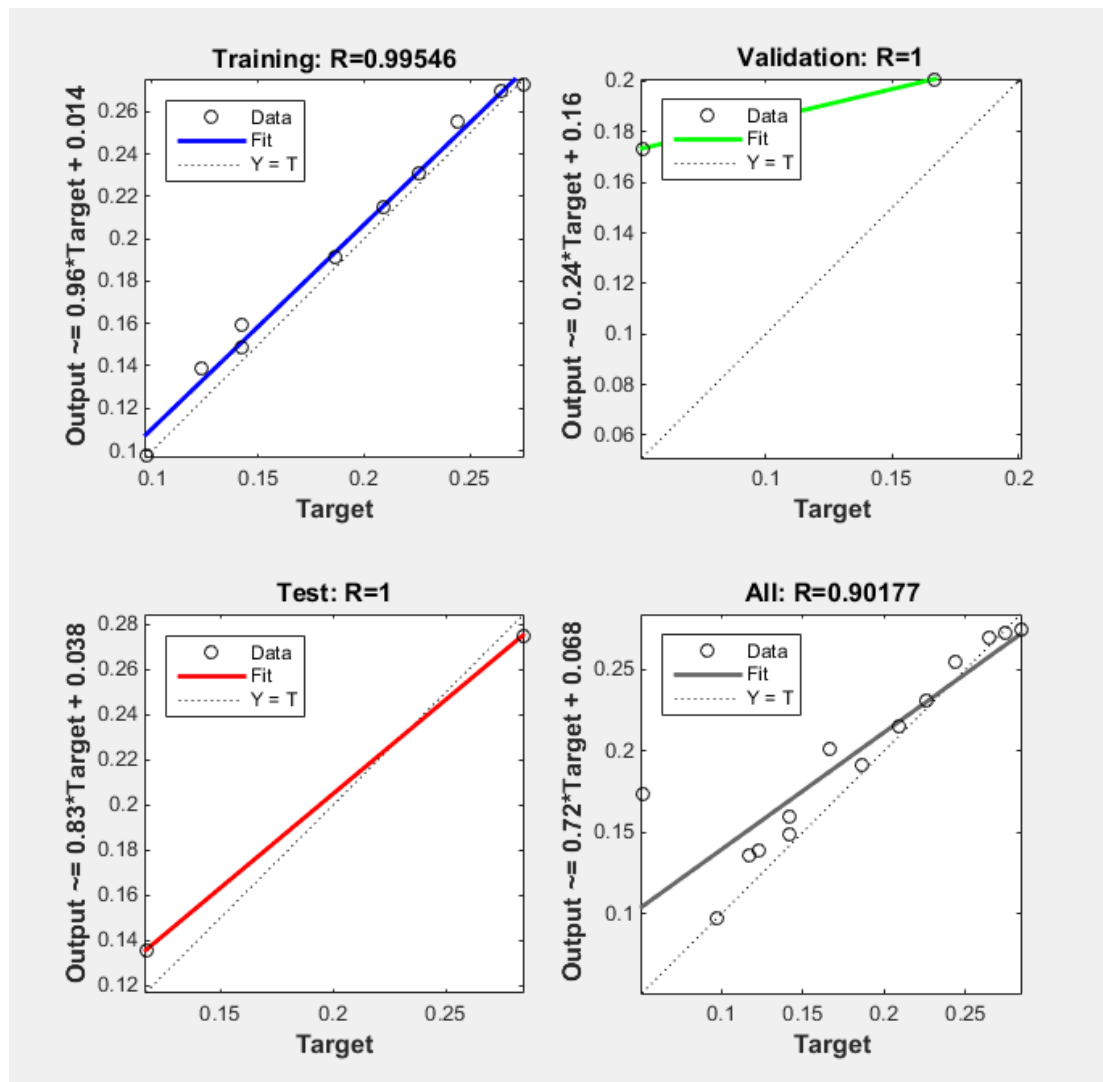

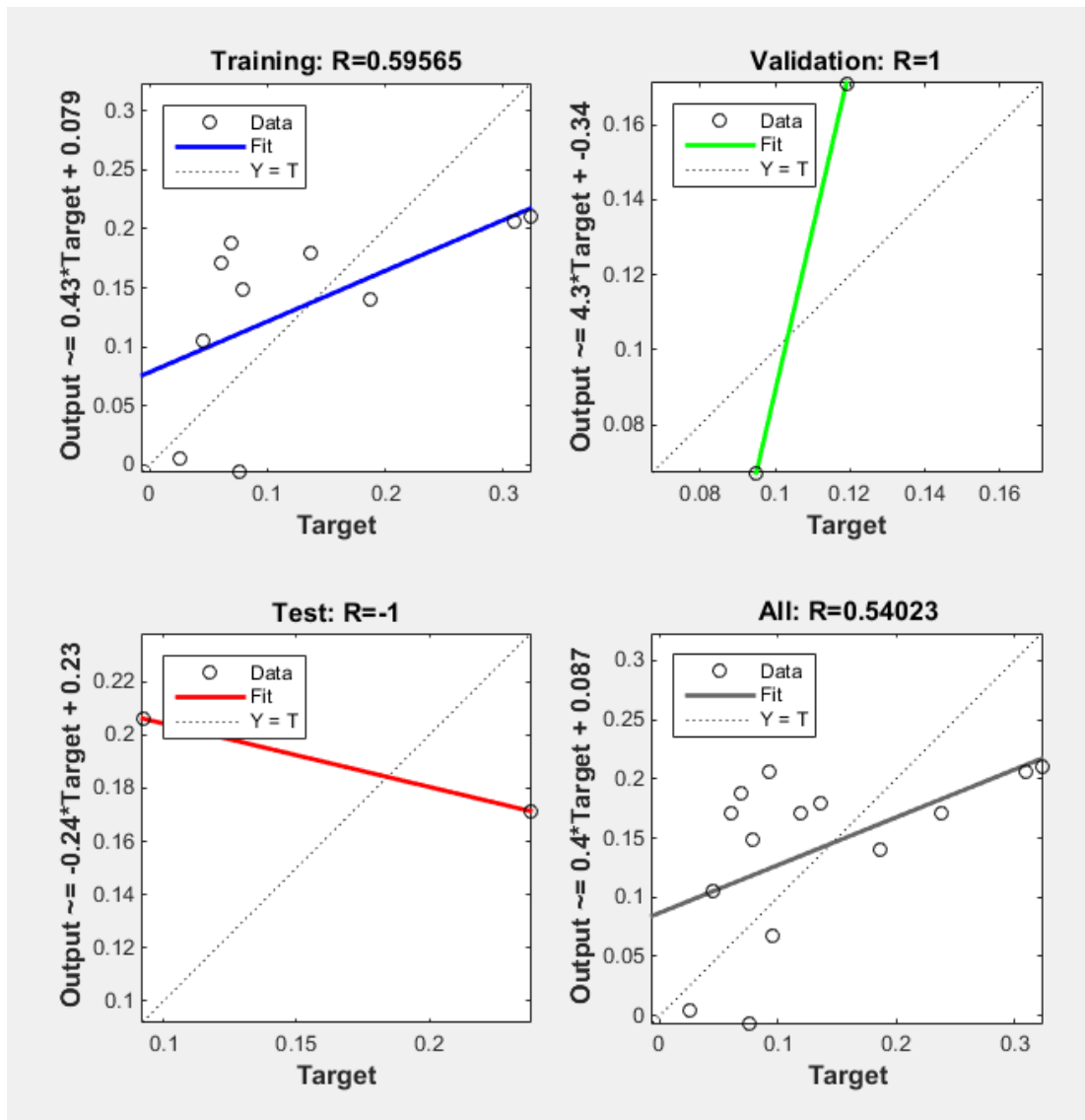Figure 4.4.1: Regression Analysis for Upstream Data Type B Swale

Figure 4.4.2: Regression Analysis for Downstream Data Type B Swale

Figure 4.4.3: MSE and R² Results for Type B Swale Downstream Data

It is shown in Figure 4.4.2 and Figures 4.4.3 that the MSE and R^2 are within the limit set in section 2.0 above. The result shows that the MSE is indeed approaching to zero and the Coefficient of Determination, R^2 is approaching to one. Hence, the data collection is reliable and considered good to be interpreted.

4.5 Regression Analysis for Both Type C Upstream and Downstream Data

Regression analysis is the statistical modeling of a range of data and to prove that the data is within the limit of Root Mean Square Error and Coefficient of Determination, R^2. It is known that a good data should have Coefficient of Determination, R^2 approaching to 1. From the Regression Analysis done by Matlab using Artificial Neural Network, the average Coefficient of Determination, R^2 for Upstream Data is $R^2 = 0.99546$
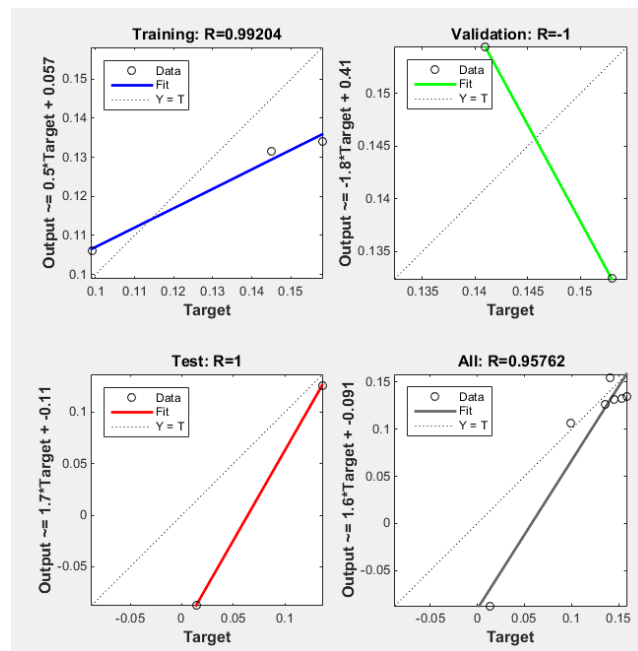

Figure 4.5.1: Regression Analysis for Upstream Data Type C Swale

Figure 4.5.2: MSE and R^2 Results for Type C Swale Upstream Data

It is shown in Figure 4.5.2 and Figures 4.5.3 that the MSE and R^2 are within the limit set in section 2.0 above. The result shows that the MSE is indeed approaching to zero and the Coefficient of Determination, R^2 is approaching to one. Hence, the data collection is reliable and considered good to be interpreted.

From the Regression Analysis done by Matlab using Artificial Neural Network, the average Coefficient of Determination, R^2 for Downstream Data is $R^2 = 0.99162$.
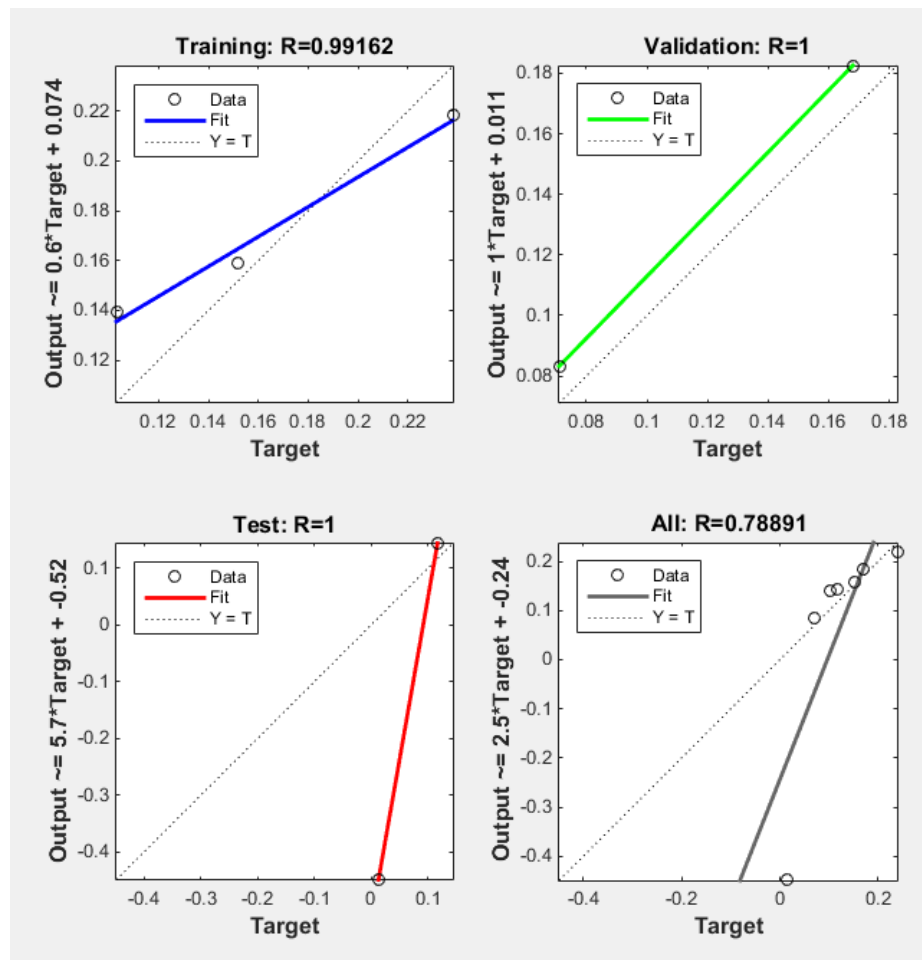

Figure 4.5.3: Regression Analysis for Downstream Data Type C Swale

Figure 4.5.4: MSE and R^2 Results for Type C Swale Downstream Data

It is shown in Figure 4.5.2 and Figures 4.5.3 that the MSE and R^2 are within the limit set in section 2.0 above. The result shows that the MSE is indeed approaching to zero and the Coefficient of Determination, R^2 is approaching to one. Hence, the data collection is reliable and considered good to be interpreted.

4.6 Prediction of Manning Roughness Coefficient for Upstream Type B Swale

From observation in Figure 4.6.1 below, it is shown that the best value is during the validation process. Artificial Neural Network does not possess the capability to train the data so that it reached the optimum performance and value for the training process. This is due to the lack of Type B Grass Swale Upstream Data.
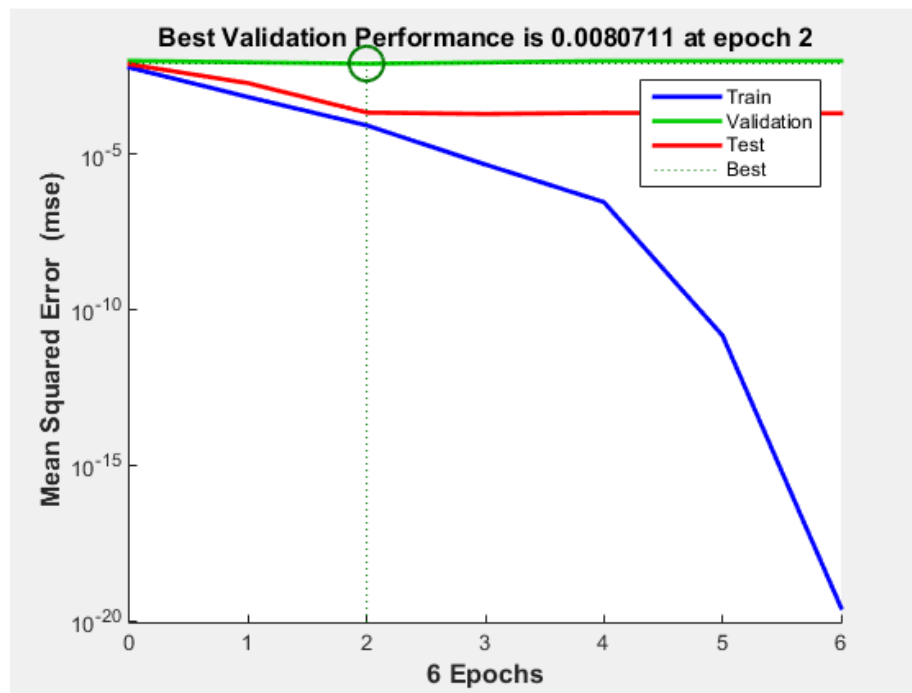

Figure 4.6.1: Best Validation Performance Graph for Upstream Type B Swale

After 6 iterations, the Artificial Neural Network stop its analysis process and rate the performance as $2.65e^{-20}$ that is approaching to zero with validation checks of 4 out of 6 as shown in Figure 4.6.2 below.
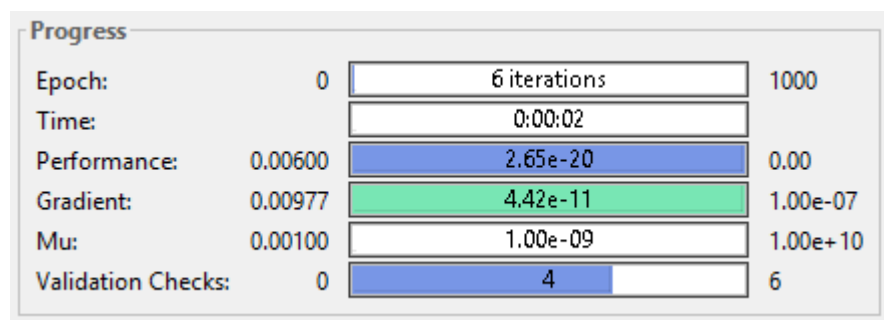

Figure 4.6.2: Progress of Artificial Neural Network Analysis for Upstream Type B Swale

Artificial Neural Network also reported that as shown in Figure 4.6.3 below that the error of the result can be as high as 0.005669 and as low as -0.1191. The prediction, however, does not show significant differences between the actual and the prediction as shown in Table 4.6.4.
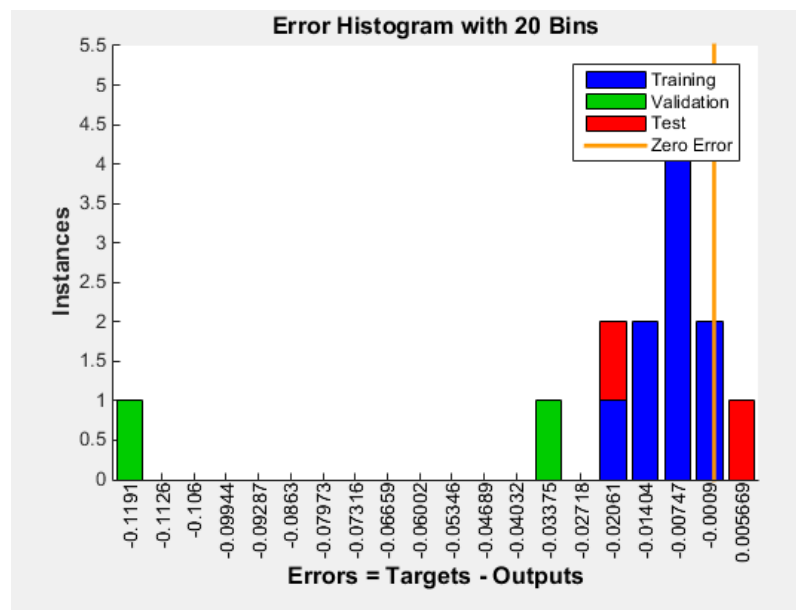

Figure 4.6.3: Histogram Error in Artificial Neural Network for Upstream Type B Swale

Upstream in Swale Type B	
Manning Roughness Coefficient, n	Predicted Manning Roughness Coefficient, n
0.051	0.173
0.123	0.139
0.186	0.191
0.275	0.273
0.244	0.255
0.265	0.270
0.117	0.136
0.142	0.159
0.142	0.149
0.167	0.201
0.284	0.275
0.226	0.231
0.097	0.098
0.209	0.215

Table 4.6.4: Comparison of Actual Manning Roughness Coefficient with the Predicted Manning Roughness Coefficient in Upstream Data of Type B Swale
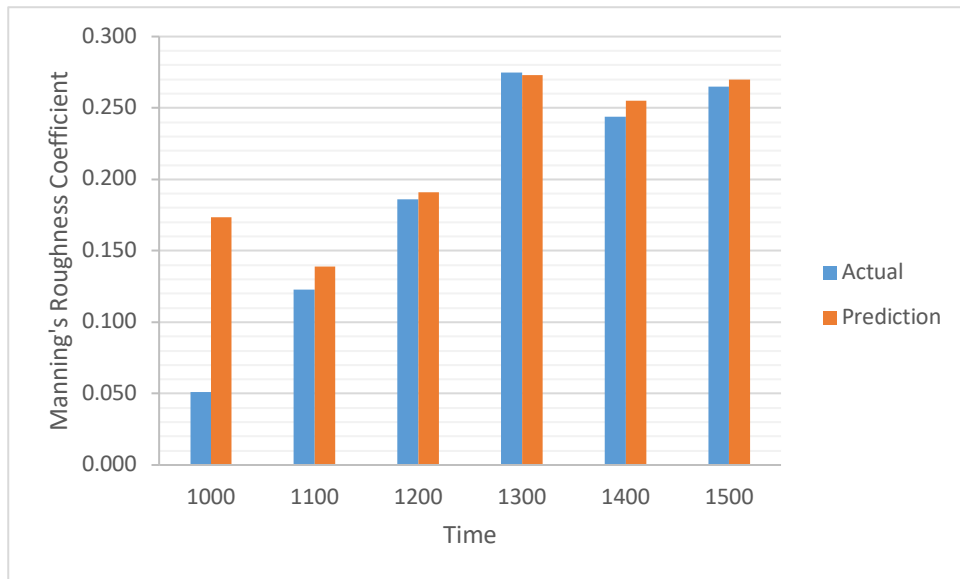
Figure 4.6.5: Difference between actual and predicted Manning's Roughness
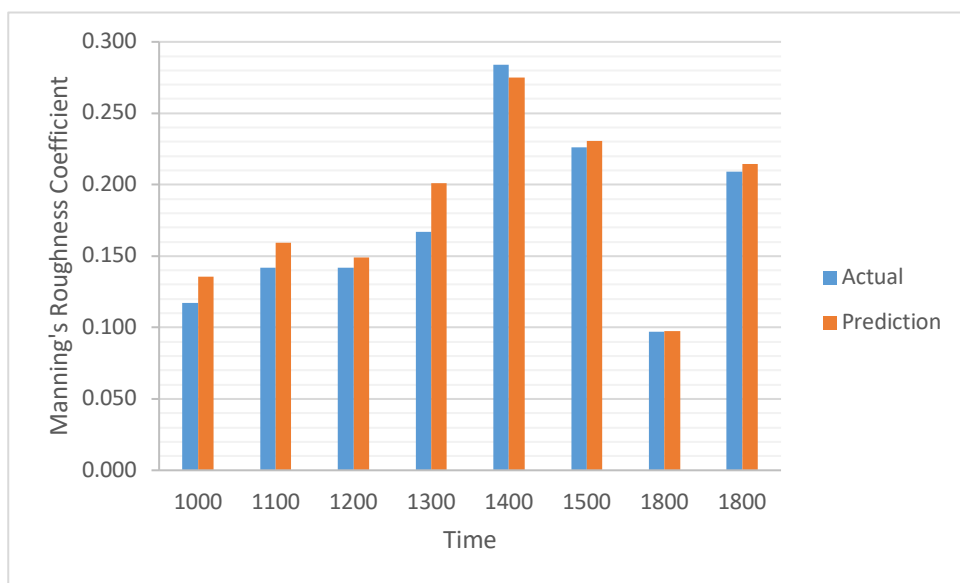Coefficient for Upstream Type B Swale in Day one

Figure 4.6.6: Difference between actual and predicted Manning's Roughness
Coefficient for Upstream Type B Swale in Day two

Both figures above shows low differentiation and variances due to the high accuracy
of ANN as compared to downstream Manning's Roughness Coefficient value of Type
B natural vegetated channel. The reason of such high accuracy value is due to the
minimum effect of natural vegetation blockade effect to the watercourse causes the
Manning's Roughness Coefficient to be less variable as compared to the Downstream
value.

Nonetheless, the RMSE and R^2 value is acceptable in this experiment and therefore the predicted value of Manning's Roughness Coefficient is considered sufficient to verify that the ANN is correct and does not lead to a misperception of this research. The value of inaccuracy can be further improved by having greater sets of data for all ANN modeling i.e. training, testing, and validation.

4.7 Prediction of Manning Roughness Coefficient for Downstream Type B Swale

From observation in Figure 4.7.1 below, it is shown that the best value is the validation and testing processes. Artificial Neural Network does not possess the capability to train the data so that it reached the optimum performance and value for the training process. This is due to the lack of Type B Grass Swale Downstream Data.
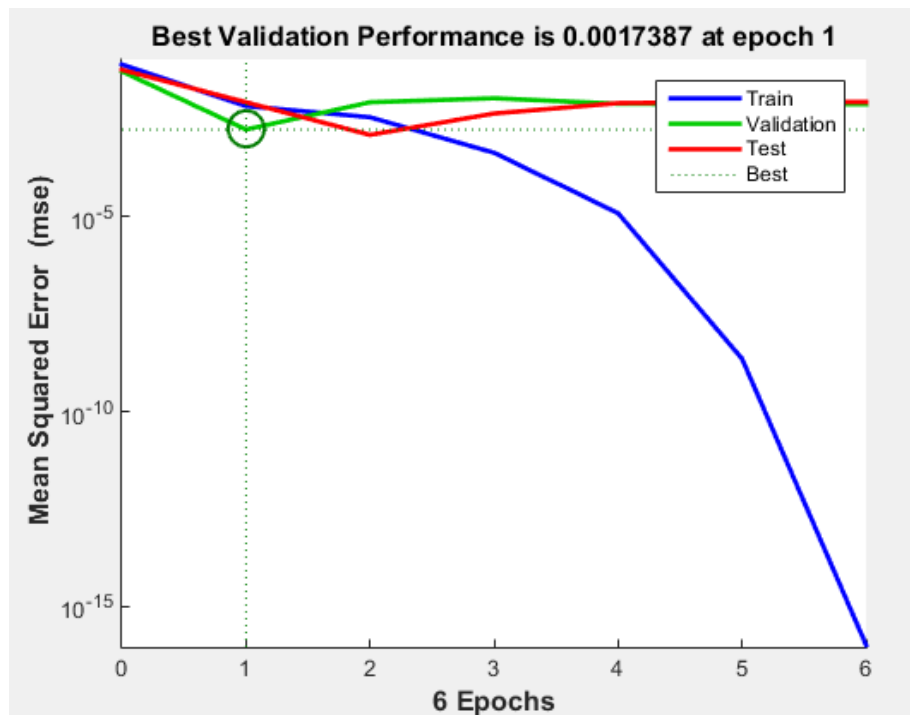

Figure 4.7.1: Best Validation Performance Graph Downstream Type B Swale

After 6 iterations, the Artificial Neural Network stop its analysis process and rate the performance as $1.01e^{-16}$ that is approaching to zero with validation checks of 5 out of 6 as shown in Figure 4.7.2 below.
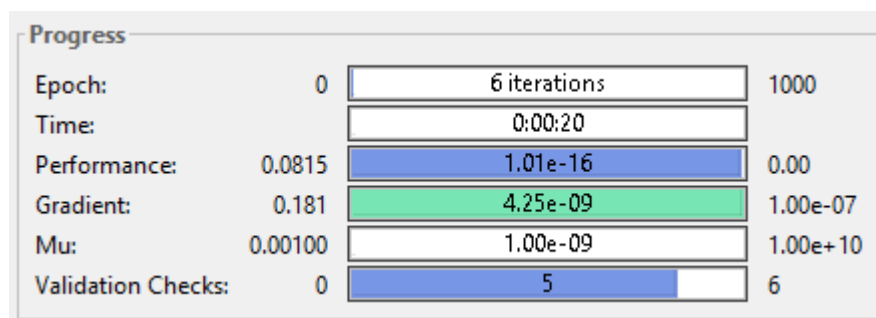

Figure 4.7.2: Progress of Artificial Neural Network Analysis Downstream Type B Swale

Artificial Neural Network also reported that as shown in Figure 4.7.3 below that the error of the result can be as high as 0.1067 and as low as -1136. The prediction, however, does not show significant differences between the actual and the prediction as shown in Table 4.7.4.
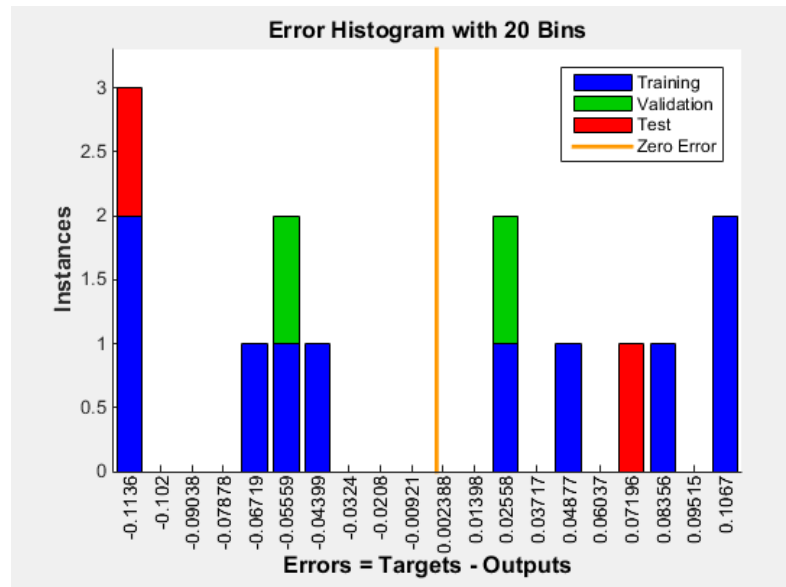

Figure 4.7.3: Histogram Error in Artificial Neural Network for Downstream Type B Swale

Downstream in Swale Type B	
Manning Roughness Coefficient, n	Predicted Manning Roughness Coefficient, n
0.025	0.005
0.069	0.188
0.060	0.171
0.079	0.148
0.076	-0.006
0.095	0.067
0.119	0.171
0.092	0.206
0.310	0.206
0.323	0.210
0.238	0.171
0.187	0.141
0.045	0.106
0.136	0.179

Table 4.7.4: Comparison of Actual Manning Roughness Coefficient with the Predicted Manning Roughness Coefficient in Downstream Data of Type B Swale
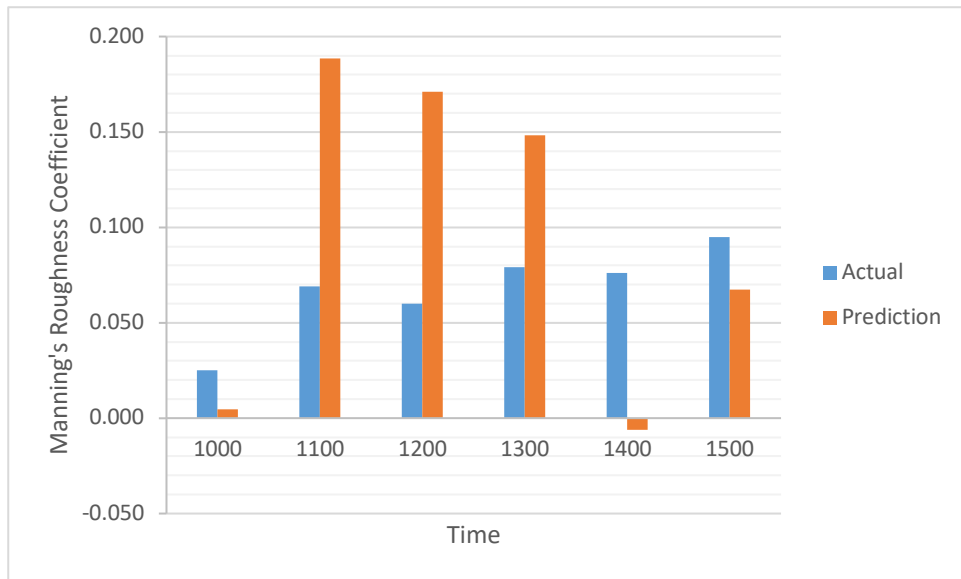
Figure 4.7.5: Difference between actual and predicted Manning's Roughness
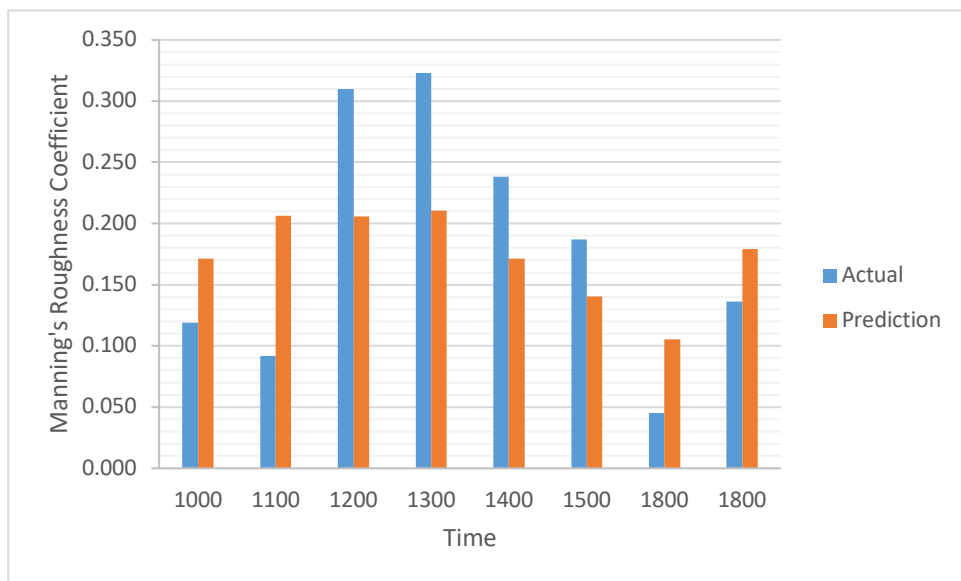Coefficient for Downstream Type B Swale in Day one

Figure 4.7.6: Difference between actual and predicted Manning's Roughness
Coefficient for Downstream Type B Swale in Day two

Both figures above shows high differentiation and variances due to the inaccuracy of
the computation modeling ANN. Nonetheless, the RMSE and R^2 value is acceptable
in this experiment and therefore the predicted value of Manning's Roughness
Coefficient is considered sufficient to verify that the ANN is correct and does not lead
to a misperception of this research. The value of inaccuracy can be further improved
by having high sets of data for all ANN modeling i.e. training, testing, and validation.

4.8 Prediction of Manning Roughness Coefficient for Upstream Type C Swale

From observation in Figure 4.8.1 below, it is shown that the best value is the validation and training processes. Artificial Neural Network does not possess the capability to train the data so that it reached the optimum performance and value for the training process. This is due to the lack of Type C Grass Swale Upstream Data.
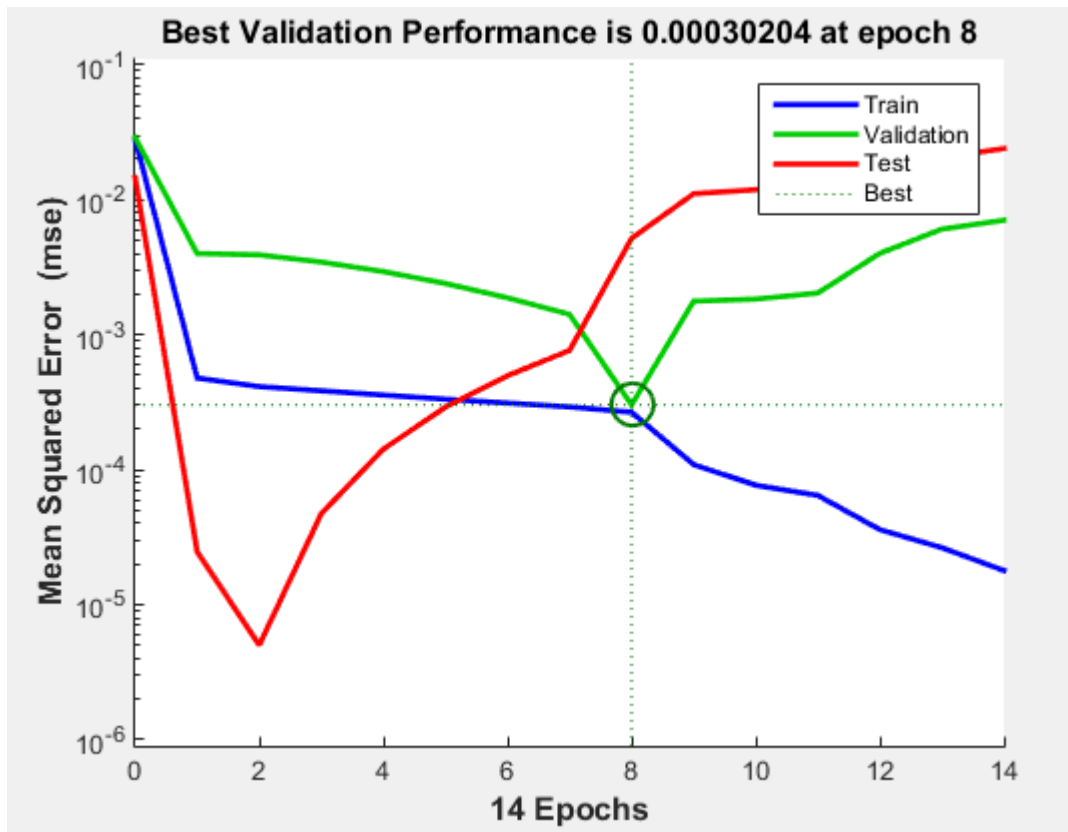

Figure 4.8.1: Best Validation Performance Graph for Upstream Type C Swale

After 14 iterations, the Artificial Neural Network stop its analysis process and rate the performance as $1.79e^{-05}$ that is approaching to zero with validation checks of 6 out of 6 as shown in Figure 4.8.2 below.
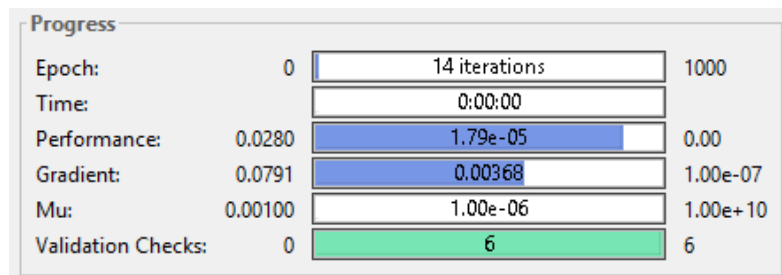

Figure 4.8.2: Progress of Artificial Neural Network Analysis for Upstream Type C Swale

Artificial Neural Network also reported that as shown in Figure 4.8.3 below that the error of the result can be as high as 0.1067 and as low as -1136. The prediction, however, does not show significant differences between the actual and the prediction as shown in Table 4.8.4.
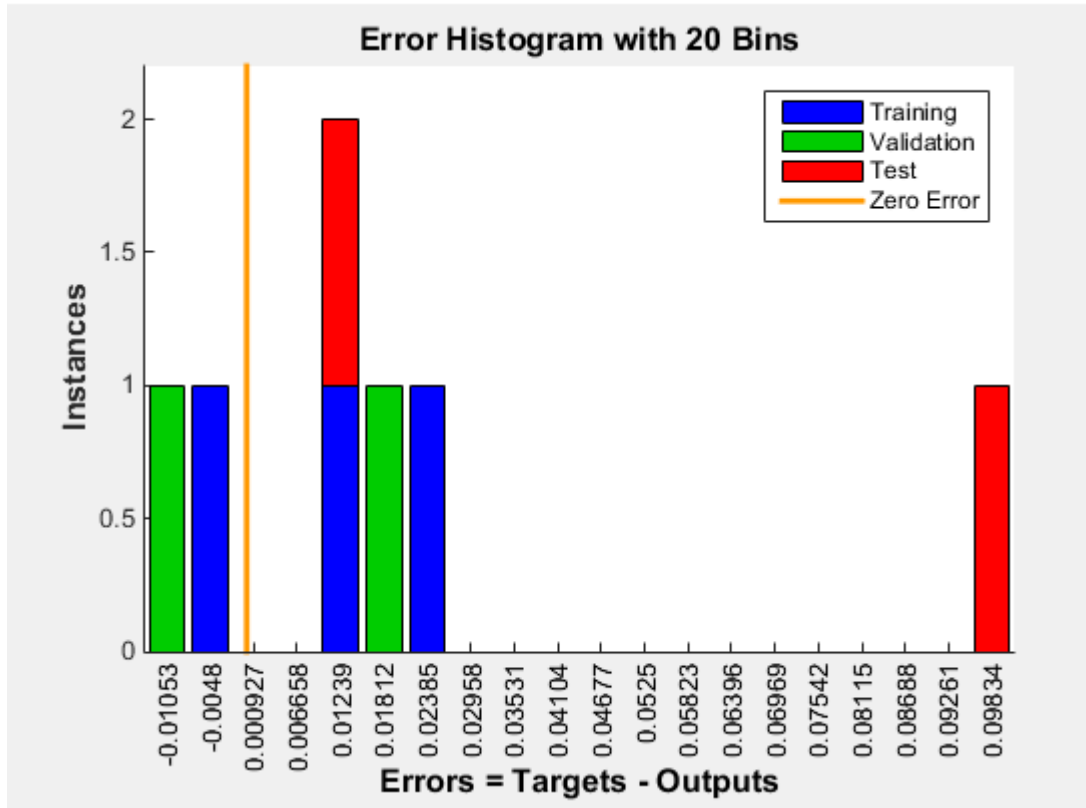
Figure 4.8.3: Histogram Error in Artificial Neural Network for Upstream Type C Swale

Upstream in Swale Type C	
Manning Roughness, n	Predicted Manning Roughness, n
0.099	0.106
0.136	0.126
0.153	0.132
0.158	0.134
0.141	0.154
0.145	0.132
0.014	-0.087

Table 4.8.4: Comparison of Actual Manning Roughness Coefficient with the Predicted Manning Roughness Coefficient in Upstream Data of Type C Swale

Figure 4.8.5: Difference between actual and predicted Manning's Roughness Coefficient in Upstream Type C Swale
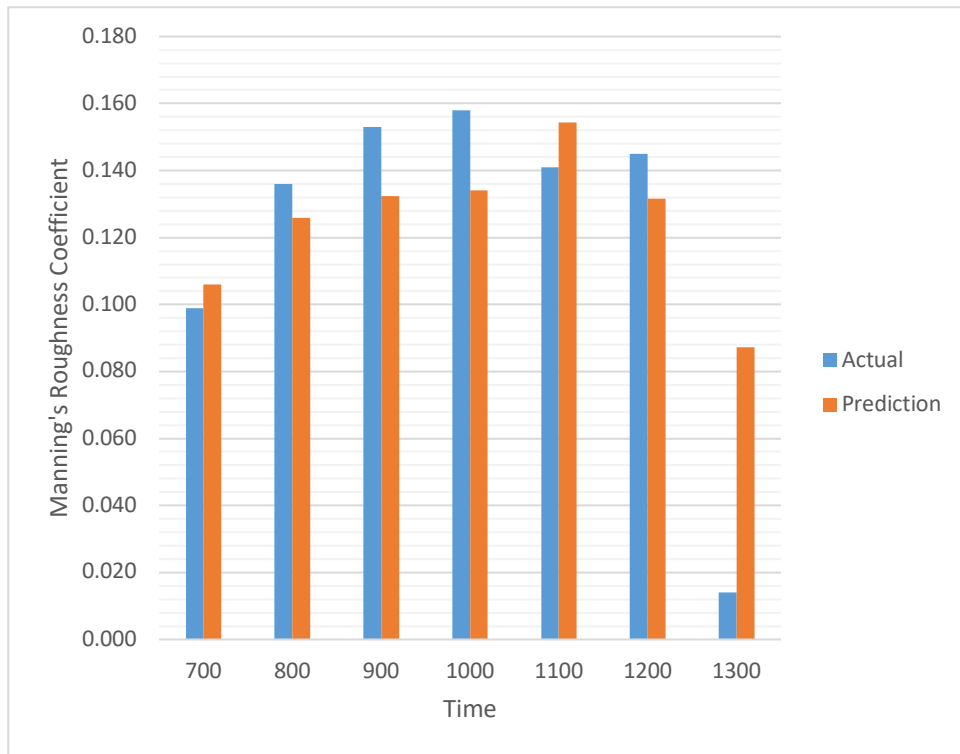
From the graph above, it shows that the Type C Swale has almost similar Manning's Roughness Coefficient for both actual and predicted values. The similarities were due to the submergence of vegetation causes the Manning's Roughness Coefficient to be similar for both upstream and downstream value. Hence, the computation modeling can be done quite easy without any improvement to a number of hidden layers needed. Nonetheless, outliers are bound to posess within the experiment due to the lack of data, especially for Type C Swale.

4.9 Prediction of Manning Roughness Coefficient for Downstream Type C Swale

From observation in Figure 4.9.1 below, it is shown that the best value is the validation and training processes. Artificial Neural Network does not possess the capability to train the data so that it reached the optimum performance and value for the training process. This is due to the lack of Type C Grass Swale Upstream Data.
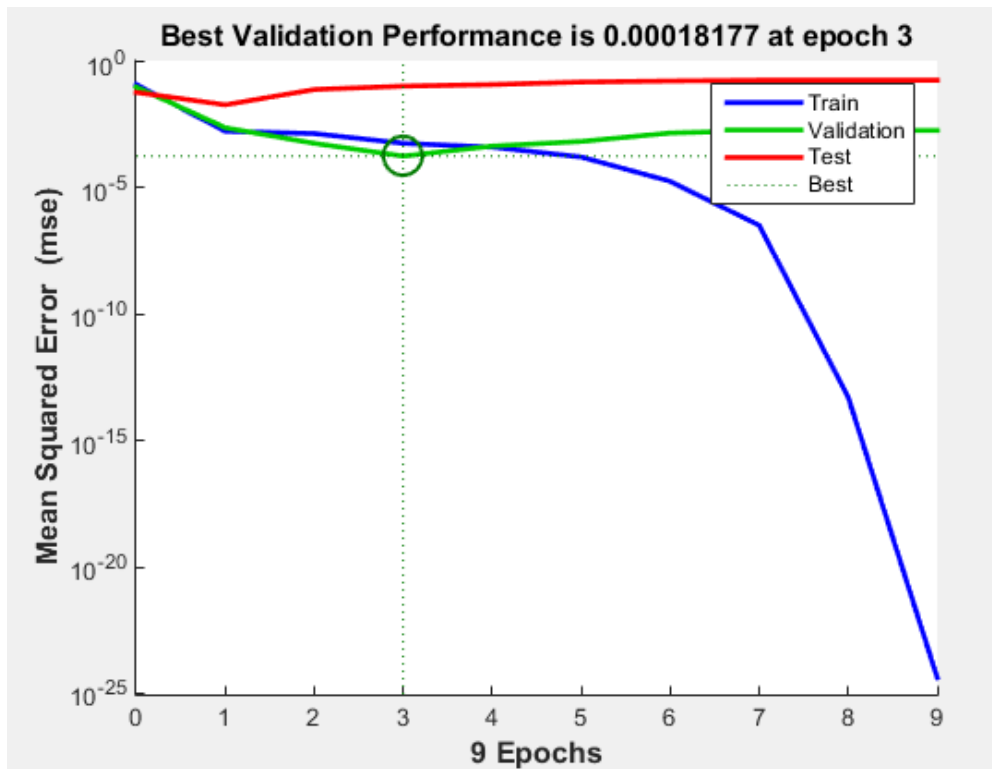

Figure 4.9.1: Best Validation Performance Graph for Downstream Type C Swale

After 9 iterations, the Artificial Neural Network stop its analysis process and rate the performance as $4.12e^{-25}$ that is approaching to zero with validation checks of 6 out of 6 as shown in Figure 4.9.2 below.
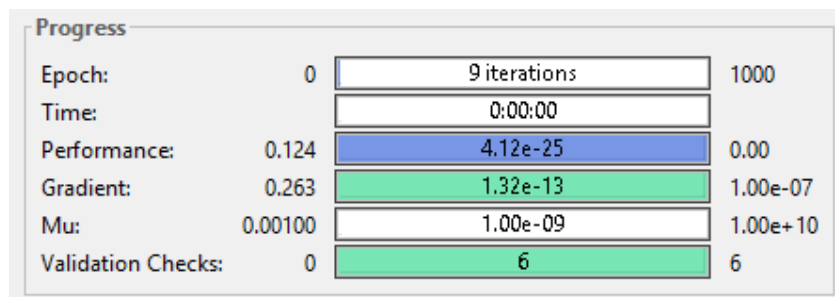

Figure 4.9.2: Progress of Artificial Neural Network Analysis for Downstream Type C Swale

Artificial Neural Network also reported that as shown in Figure 4.9.3 below that the error of the result can be as high as 0.4494 and as low as -0.02392. The prediction, however, does not show significant differences between the actual and the prediction as shown in Table 4.9.4.
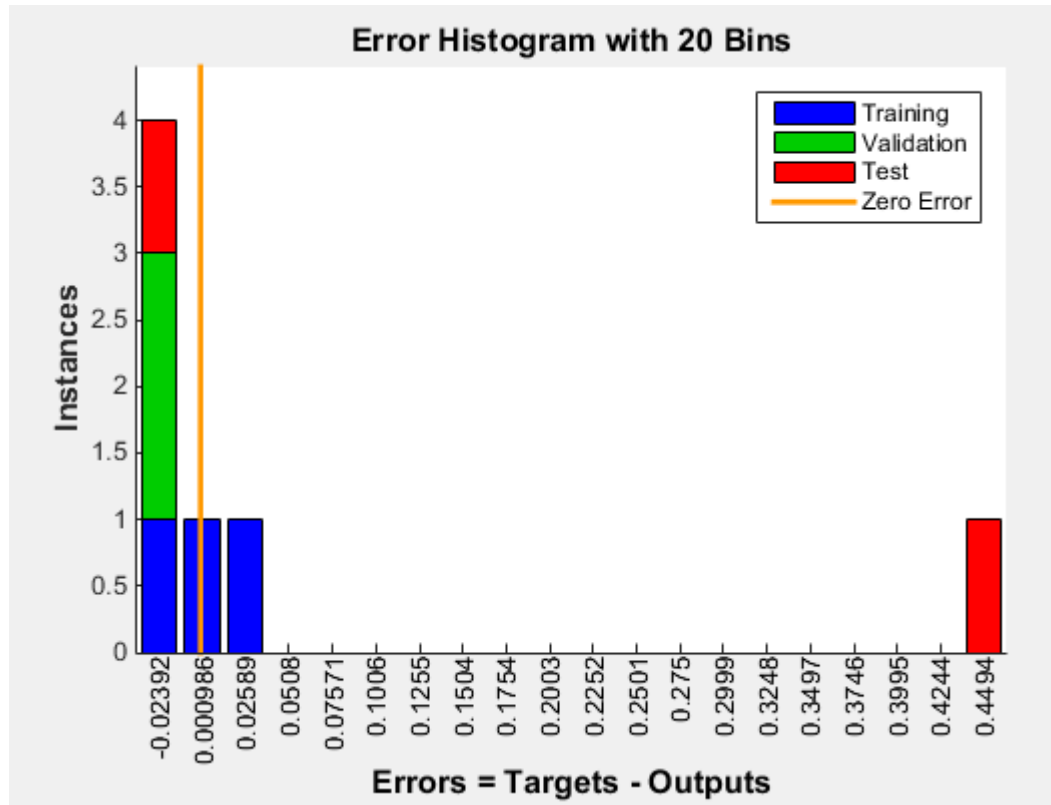
Figure 4.9.3: Histogram Error in Artificial Neural Network for Downstream Type C Swale

Downstream in Swale Type C	
Manning Roughness, n	Predicted Manning Roughness, n
0.071	0.083
0.103	0.139
0.117	0.144
0.168	0.183
0.238	0.218
0.152	0.159
0.013	-0.449

Table 4.9.4: Comparison of Actual Manning Roughness Coefficient with the Predicted Manning Roughness Coefficient in Upstream Data of Type C Swale
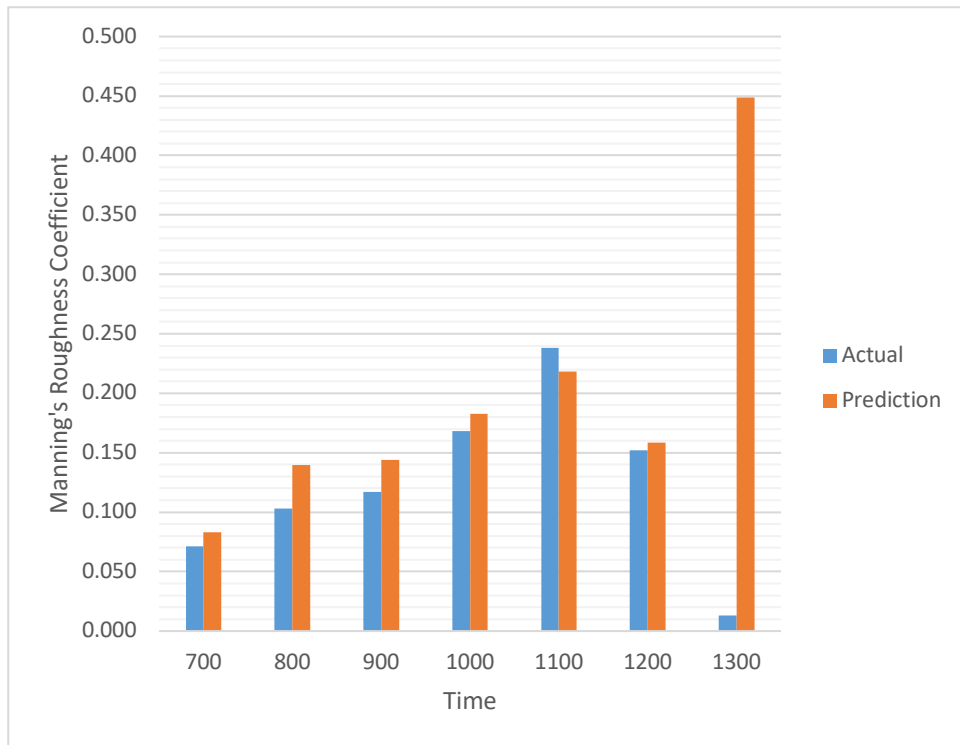
Figure 4.9.5: Difference between actual and predicted Manning's Roughness
Coefficient in Downstream Type C Swale

From the graph above, it shows that the Type C Swale has almost similar Manning's Roughness Coefficient for both actual and predicted values. The similarities were due to the submergence of vegetation causes the Manning's Roughness Coefficient to be similar for both upstream and downstream value. Hence, the computation modeling can be done quite easy without any improvement to a number of hidden layers needed. Nonetheless, outliers are bound to have in the experiment due to the lack of data, especially for Type C Swale.

5.0 Conclusion and Recommendation

As a conclusion, a more controlled experiment data can be done in the laboratory using hydraulics flume. The installation of the vegetation should also be carefully determined by referring to the previous bioengineering techniques when simulating and establishing a naturally vegetated channel. Every procedure is then recorded and a standard experimental procedure is established after the setting up of the vegetated flume is satisfied.

The differences of cross section between Swale Type B and Swale Type C definitely resulted to different Manning Roughness Coefficient, n. The reading shows that the most optimum type of swale would be Type B swale where the Roughness Manning Coefficient, n can be as high as 0.310. Water flow in Type C swale has a tendency to submerge the vegetation due to its high depth. Therefore, resulted to fair amount of Manning Roughness Coefficient throughout the naturally vegetated channel for both Upstream and Downstream region.

Hence, optimization of the naturally vegetated channel can be further research by studying the effect of flow velocity and Manning Roughness Coefficient to the length of the vegetation. It is also proven that the prediction of Flow Resistance can be made and analysis by the Artificial Neural Network tool. The results shown in section 4.0 prove that the predicted Manning Roughness Coefficient n is more or less the same as the actual Manning Roughness Coefficient, n that has been calculated using Manning Roughness Coefficient as explained in section 2.0.

However, it is also observed that lack of data resulted in low efficiency in performance of the Artificial Neural Network as per predicted in Type C Swale. Therefore, gaining more data will be able to ensure the accuracy of the performance of the Artificial Neural Network giving a more accurate result and prediction.

The author recommendation in this research would be to observe the reaction of the velocity of the water flow with a different arrangement of vegetation. The optimum flow resistant could also be obtained with a different way of arranging the vegetation in the flume. Such, different arrangement will give a greater insight whether the

arrangement of vegetation will either reduce or increase the flow velocity of any given flow rate.

Besides that, future extensive research could also be made in order to study the effects of the naturally vegetated channel to the concentration of oxygen in the outflow of the water discharged. With the extensive research, the naturally vegetated channel could also be proven as one inexpensive medium to reduce pollution up to a certain degree in the drainage system in Malaysia. Thus, increase the poor state of Malaysia's river in terms of pollution.

6.0 References

1. Yatim, B., Toriman, M. E., Maimon, A., Surif, S., Chen, C. Y., & Lee, Y. H. (2013). The impact of climate change on flood risk in the muar river basin of Malaysia. *Disaster Advances*, *6*(10), 11-17.

2. Gang, C. H. E. N., HUAI, W. X., Jie, H. A. N., & ZHAO, M. D. (2010). Flow Structure in Partially Vegetated Rectangular Channels. *Journal of Hydrodynamics, Ser. B*, *22*(4), 590-597.

3. *Open Channel Flow: Uniform Flow, best hydraulic sections, energy principles, Froude Number*. Retrieved on June 20, 2016, at mimosa website: http://mimoza.marmara.edu.tr/~neslihan.semerci/ENVE204/L9.pdf

4. Sand-Jensen, K. (2003). Drag and reconfiguration of freshwater macrophytes. *Freshwater Biology*, *48*(2), 271-283.

5. KEE, L. C., ZAKARIA, N. A., LAU, T. L., CHANG, C. K., & GHANI, A. A. Determination of manning's n for the subsurface modular channel.

6. Muravyev, N. V., & Pivkina, A. N. (2016). NEW CONCEPT OF THERMOKINETIC ANALYSIS WITH ARTIFICIAL NEURAL NETWORKS.*Thermochimica Acta*.

7. Vuik, V., Jonkman, S. N., Borsje, B. W., & Suzuki, T. (2016). Nature-based flood protection: The efficiency of vegetated foreshores for reducing wave loads on coastal dikes. *Coastal Engineering, 116*, 42-56.

8. Thorndah S. &Willems P. 2008. Probabilistic modeling of overflow, surges and flooding in urban drainage using the 1st order reliability method and parameterization of local rain series. Water research, 42(1-2), 455-466.

9. Kong Yoke Yoon, Noor AzimaBintiBahrun, and Yew Kun.A study on the urban flooding. October 2010.

6.0 Appendices

Figure 6.1: Type B Swale

Figure 6.2: Type B Swale

Figure 6.3: Type C Swale

Figure 6.4: Type C Swale